Geometric Methods for Finite Rational Inattention

Roc Armenter*, Michèle Müller-Itten†, Zachary R. Stangebye‡

September 13, 2023

Abstract

We present a geometric approach to the finite Rational Inattention (RI) model, recasting it as a convex optimization problem with reduced dimensionality that is well-suited to numerical methods. We provide an algorithm that outperforms existing RI computation techniques in terms of both speed and accuracy in both static and dynamic RI problems. We further introduce methods to quantify the impact of numerical inaccuracy on the model's outcomes and to produce robust predictions regarding the most frequently implemented actions.

Keywords: Rational inattention, Shannon entropy, information acquisition, learning, consideration sets.

JEL: D81, D83, C63

*Federal Reserve Bank of Philadelphia: roc.armenter@phil.frb.org

†University of St. Gallens: michele.mueller-itten@unisg.ch

‡University of Notre Dame: zstangeb@nd.edu

The views expressed in this paper are solely those of the authors and do not necessarily reflect the views of the Federal Reserve Bank of Philadelphia or the Federal Reserve System. The authors would like to thank Isaac Baley, Thomas Gresik, Maciej Kotowski, John Leahy, Filip Matějka, Jun Nie, and participants at various conferences and seminars for constructive feedback and comments. Financial support from the Notre Dame Institute for Scholarship in the Liberal Arts is gratefully acknowledged. Philadelphia Fed working papers are free to download at https://philadelphiafed.org/research-and-data/publications/working-papers.

1 Introduction

Introduced by Sims [2003], Rational Inattention (RI) has been gaining increased acceptance as a model of information acquisition and processing, particularly in macroeconomics and finance. However, by and large we still do not know how effective RI models are at explaining real-world phenomena. Maćkowiak et al. [2023, p.27] states that "the model of RI is well suited for a boom in empirical work, which has not yet occurred," and Gabaix [2014] notes that the limited scope of existing applied work is partly due to the conceptual and computational complexity of RI optimization problems. Outside of a handful of special cases, RI models do not admit a closed-form solution. Existing numerical methods are often computationally intensive and may suffer from accuracy problems.

We introduce a geometric approach to finite RI models with the most common information cost specification, the average reduction in Shannon entropy [Caplin et al., 2018, Matějka and McKay, 2015, Sims, 2003]. Our approach is very well suited for numerical computation, simplifying the original problem and providing novel methods to quantify the accuracy of its behavioral predictions.

To obtain the geometric approach, we introduce a simple mapping from state-dependent payoffs into what we term 'attention vectors' — the mapping accentuates payoff differences when information is cheap and attenuates them when it is expensive. When applied to the action payoffs of an RI problem, the resulting attention vectors span a convex polytope, the 'attention possibilities set.' The original RI problem is then equivalent to finding the optimal attention vector from this set, resulting in a strictly convex optimization problem. This geometric approach is markedly simpler, reducing the dimensionality of the original problem, providing two sets of convenient optimality conditions, and separating the roles of prior beliefs and payoffs. Yet, it

is straightforward to recover the joint probability distribution of states and actions from the optimal attention vector.

There are several algorithms for convex optimization problems that can be readily used for our geometric approach. We provide one such algorithm, adapted from standard sequential quadratic programming with active set methods.[1] Our algorithm performs favorably compared with other approaches, delivering substantial gains in both speed and accuracy. The geometry of the attention vectors informs three noteworthy design features: Our choice of active sets, the stopping criterion, and a scaling routine to avoid floating point errors.

We also provide novel methods designed to improve the accuracy and robustness of the behavioral predictions of the model's numerical solutions. We first propose a precision metric that relies on the similarity of the implied attention vectors and ensures that the joint distribution of states and actions converges to the true solution. It does so by balancing tolerance errors on two margins: The extensive margin that identifies *which* actions are chosen with positive probability, and the intensive margin that specifies the relative frequency of each chosen action. The set of actions chosen with positive probability, also known as the 'consideration set', is often an object of interest by itself but is notoriously difficult to identify numerically.

We show how to obtain robust predictions regarding the most and least frequently implemented actions despite numerical inaccuracy. Manipulating the two optimality conditions from the geometric approach, we derive 'cover' sets of actions that, altogether, are played with an overall probability of our choice. These covers can be used either to approximate the consideration set or, conversely, to identify actions that are rarely, if ever, chosen. The latter is helpful for hypothesis testing: Identifying groups of actions that jointly have a low choice probability ensures that a rejection of the

[1]Source codes are available on GitHub at `https://github.com/mmulleri/GAP-SQP`.

underlying RI specification is not clouded by noise from the computation.

We provide a pair of applications intended to illustrate some of the advantages of our approach. The first application is based on the price-setting problem of Matějka [2016]. We document that our algorithm is orders of magnitude faster than the well-known Blahut-Arimoto algorithm [see Cover and Thomas, 2012] and scales well with the size of the action and state spaces. The superior convergence speed is maintained when the algorithm is integrated in dynamic algorithms such as the one suggested by Miao and Xing [2022]. Precision, rather than speed, is the focus of our second application, based on the two-dimensional portfolio design problem of Jung et al. [2019]. Our algorithm unveils some behavioral differences regarding the frequency and structure of portfolio rebalancing. In both applications, we obtain robust predictions by deploying our geometric methods, which provide very tight estimates of the consideration set.

Related literature. Rational inattention models have rapidly found their way into a variety of fields, from finance to monetary economics. We do not aim to properly review what is by now a large literature — see Maćkowiak et al. [2023] for an excellent survey of both theoretical and applied work with RI models. Instead we briefly discuss previous key developments in solution methods for RI models.

Early work on RI models restricted analysis to Linear-Quadratic Gaussian (LQG) frameworks, or assumed that the solution was Gaussian as an approximation, to obtain analytic results that can, in turn, be embedded in an equilibrium model and have led to many insights for aggregate phenomena.[2]

Sims [2006] exhorted researchers to go beyond the LQG case, and more recent

[2] A necessarily incomplete list of examples is: Peng [2005], Peng and Xiong [2006], and Huang and Liu [2007] for asset pricing; Maćkowiak and Wiederholt [2009] for monetary shocks; Gaglianone et al. [2020] for forecasting; Van Nieuwerburgh and Veldkamp [2009] and Van Nieuwerburgh and Veldkamp [2010] for home bias and under-diversification in asset portfolios.

research has addressed some of the shortcomings of the LQG framework: Luo et al. [2017] apply Gaussian techniques with constant absolute risk aversion preferences, allowing them to study the dynamics of consumption and wealth in general equilibrium. Mondria [2010] allows signals to be linear combinations of the underlying state of the economy, an approach that is also followed in Kacperczyk et al. [2016], among others. Miao et al. [2022] make further progress in multi-variate LQG environments. In settings where choices are discrete, some researchers use the Cardell distribution to obtain closed forms that are amenable to empirical analysis [Bertoli et al., 2020, Brown and Jeon, 2023, Dasgupta and Mondria, 2018].

Our methods offer an alternative to these distributional form assumptions, for problems with finitely many states and actions. While many of the RI problems in finance and macroeconomics feature a continuum of actions and states, the computational gains of our approach make it feasible to use very fine grids. Our applications in Sections 5.1 and 5.2 draw on two leading examples that apply such discretization to continuous problems, Matějka [2016] and Jung et al. [2019].

Paper structure. We formally describe the classic Rational Inattention approach in Section 2 and introduce our geometric approach in Section 3. In Section 4, we develop a toolkit for finite RI problems that improve the accuracy and robustness of numerical methods. Section 5 illustrates the relevance of these new tools in three specific applications, and Section 6 concludes.

Notation. We use vector notation throughout the paper and rely on the following conventions: Boldface letters such as $\boldsymbol{x}$ denote I-dimensional vectors. To describe its component-wise construction, we also refer to $\boldsymbol{x}$ as $[x_i]$. For example, $[x_i/y_i]$ describes the vector $\boldsymbol{z}$ with i-th component $z_i = x_i/y_i$. When comparing vectors, we

write $\boldsymbol{x} \geq \boldsymbol{y}$ if and only if $x_i \geq y_i$ for all i, $\boldsymbol{x} > \boldsymbol{y}$ if and only if $\boldsymbol{x} \geq \boldsymbol{y}$ and $\boldsymbol{x} \neq \boldsymbol{y}$, and $\boldsymbol{x} \gg \boldsymbol{y}$ if and only if $x_i > y_i$ for all i.

2 Rational Inattention Problem

We consider the standard RI problem where an agent faces a finite menu of options with state-dependent payoffs and can condition her choice on arbitrary but costly signals. More accurate signals are more costly, and we follow the literature [Caplin et al., 2018, Matějka and McKay, 2015, Sims, 2003, 2006] in focusing on information-processing costs that are proportional to Shannon entropy.

Formally, an agent faces an unknown state of the world $i \in \mathcal{I} = \{1, ..., I\}$, each occurring with positive *prior* probability $\pi_i > 0$. The agent has to implement a single *action* $\boldsymbol{a}$ from the finite *menu* $\mathcal{A}$. Each action is written as a payoff vector $\boldsymbol{a} = (a_1, ..., a_I) \in \mathbb{R}^I$, with a_i describing the agent's resulting utility if she ends up implementing action $\boldsymbol{a}$ in state i. We denote the set of probability mass functions over the menu as $\Delta\mathcal{A}$. Before implementing an action, the agent can acquire information about the state of the world, but more accurate information is more costly. By the obedience principle [Bergemann and Morris, 2016], it is without loss of generality to assume that the decision maker relies on a signal that directly recommends a specific action. We denote the resulting conditional implementation probabilities by $\boldsymbol{P} \in (\Delta\mathcal{A})^I$, where $P_i(\boldsymbol{a})$ denotes the probability of implementing action $\boldsymbol{a}$ conditional on state i.

The optimal conditionals $\boldsymbol{P}$ maximize expected consumption utility net of information processing costs. Expected consumption utility can be stated succinctly as $\sum_{i\in\mathcal{I}} \pi_i \sum_{\boldsymbol{a}\in\mathcal{A}} P_i(\boldsymbol{a}) a_i$ since actions are denoted as payoff vectors. Information processing costs are measured as the average reduction in Shannon entropy between prior

and posterior. These costs are also known as the mutual information and are equal to the expected Kullback-Leibler divergence between conditional and marginal choice probabilities [Cover and Thomas, 2012],

$$\mathsf{MI}(\boldsymbol{P}, p \,|\, \boldsymbol{\pi}) = \sum_{i \in \mathcal{I}} \sum_{\boldsymbol{a} \in A} \pi_i P_i(\boldsymbol{a}) \ln\left(\frac{P_i(\boldsymbol{a})}{p(\boldsymbol{a})}\right),$$

where $p(\boldsymbol{a}) = \boldsymbol{\pi} \cdot \boldsymbol{P}(\boldsymbol{a})$ refers to the marginal implementation probability of $\boldsymbol{a}$.[3] A proportionality constant $\lambda > 0$ translates the informational burden from nats into utils. Mathematically, the choice problem is parametrized by a triplet $(\mathcal{A}, \boldsymbol{\pi}, \lambda)$, and welfare is given by

$$W(\mathcal{A}, \boldsymbol{\pi}, \lambda) = \begin{cases} \max\limits_{\boldsymbol{P} \in (\Delta\mathcal{A})^I,\, p \in \Delta\mathcal{A}} & \sum\limits_{i \in \mathcal{I}} \pi_i \sum\limits_{\boldsymbol{a} \in \mathcal{A}} P_i(\boldsymbol{a}) a_i - \lambda\, \mathsf{MI}(\boldsymbol{P}, p \,|\, \boldsymbol{\pi}) \\ \text{s.t.} & p(\boldsymbol{a}) = \boldsymbol{\pi} \cdot \boldsymbol{P}(\boldsymbol{a}) \qquad \forall \boldsymbol{a} \in \mathcal{A}. \end{cases} \tag{RI}$$

RI agents frequently rely only on a subset of all available actions, and we follow Caplin et al. [2018] in referring to $\mathsf{support}(\boldsymbol{P})$ as the agent's 'consideration set'.

3 Geometric Approach

Key to our results is the equivalence between (RI) and a simpler optimization problem, which we call the Geometric Approach (G). To get there, we show that it is without loss of generality to relax the constraint in (RI), as the optimal marginals are always consistent with the conditionals (see Lemma 3 in the appendix). Using standard

[3] In line with conventional notation, we assume that $0 \ln 0 = 0$.

optimization techniques, we find that optimal conditionals are equal to

$$P_i(\boldsymbol{a}) = \frac{p(\boldsymbol{a})e^{a_i/\lambda}}{\sum_{\boldsymbol{a}'\in\mathcal{A}} p(\boldsymbol{a}')e^{a'_i/\lambda}}, \tag{1}$$

based on the same first-order conditions as previously reported Matějka and McKay [2015]. As observed by Caplin et al. [2018], most terms in (RI) cancel out when we substitute in these conditionals,

$$W(\mathcal{A}, \boldsymbol{\pi}, \lambda) = \lambda \max_{p\in D} \sum_{i\in\mathcal{I}} \pi_i \ln \left(\sum_{\boldsymbol{a}\in\mathcal{A}} p(\boldsymbol{a})e^{a_i/\lambda} \right), \tag{2}$$

but only a finite set of marginals $p \in D \subseteq \Delta\mathcal{A}$ is consistent with Equation (1). In our relaxed version of (RI), this restriction falls away and any marginal in $\Delta\mathcal{A}$ is feasible. The resulting maximization problem is at the heart of our approach, but for convenience we divide by the constant λ and apply a change of variables.

Specifically, we assign to each action $\boldsymbol{a}$ an *attention vector* $\boldsymbol{\beta}(\boldsymbol{a}) := [e^{a_i/\lambda}] \in (0,\infty)^I$. The mapping $\boldsymbol{\beta} : \mathbb{R}^I \to \mathbb{R}^I_{>0}$ from payoff to attention vectors accentuates differences in payoffs when the information is cheap and attenuates them when it is costly. In particular, if action $\tilde{\boldsymbol{a}}$ has a lower payoff in state i than action $\boldsymbol{a}$, the relative size of its attention vector,

$$\frac{\beta_i(\tilde{\boldsymbol{a}})}{\beta_i(\boldsymbol{a})} = e^{(\tilde{a}_i - a_i)/\lambda},$$

converges to 0 as $\lambda \to 0^+$ and 1 as $\lambda \to \infty$, so that action $\tilde{\boldsymbol{a}}$ attracts almost no attention relative to $\boldsymbol{a}$ in state i when attention costs are small, and largely equal attention when they are large.

The convex hull over all attention vectors spanned by $\mathcal{A}$,

$$\mathcal{B} := \left\{ \sum_{\boldsymbol{a} \in \mathcal{A}} p(\boldsymbol{a}) \boldsymbol{\beta}(\boldsymbol{a}) \;\middle|\; p \in \Delta\mathcal{A} \right\} \subset \mathbb{R}^I_+,$$

forms the set of feasible attention vectors or, colloquially, the 'attention possibilities set'. We assign utility $w(\boldsymbol{b}) := \boldsymbol{\pi} \cdot \ln(\boldsymbol{b})$ to each attention vector $\boldsymbol{b}$ and then solve for the most attractive, feasible attention vector by restating the relaxation of Equation (2) as

$$\max_{\boldsymbol{b} \in \mathcal{B}} w(\boldsymbol{b}). \tag{G}$$

This strictly convex optimization problem is what we call the *Geometric Approach*, or (G) for short. Figure 1 attests to why we call the approach 'geometric'. The mapping $\boldsymbol{\beta}$ transforms each available action $\boldsymbol{a}$ into an attention vector $\boldsymbol{\beta}(\boldsymbol{a})$ (drawn as black dots). Their convex hull describes the set of feasible attention vectors $\mathcal{B}$ (shaded in gray), and the indifference curves from the strictly convex utility function w (dashed lines) indicate the unique optimal attention vector $\boldsymbol{b}^*$, which always lies on the upper boundary $\partial^+\mathcal{B} = \{\boldsymbol{b} \in \mathcal{B} \mid \nexists \boldsymbol{b}' \in \mathcal{B} : \boldsymbol{b}' > \boldsymbol{b}\}$ of the feasible set (drawn in blue) due to monotonicity of w.

The geometric representation yields an immediate bound on the number of actions that the RI agent implements with positive probability.[4] The new formulation also separates the role of prior beliefs from that of payoffs: Prior $\boldsymbol{\pi}$ enters the objective function through utility w — akin to preferences — but the attention possibilities set $\mathcal{B}$ is entirely determined by the action payoffs $\boldsymbol{a}$ as well as the attention cost parameter λ. This stark split proves useful to understand how the optimal attention

[4] Carathéodory's Theorem states that at most I points are required to span any point in a $I-1$-dimensional convex hull [e.g. Eggleston, 1958, Theorem 18]. Since $\boldsymbol{b}^*$ is part of the $I-1$-dimensional upper boundary $\partial^+\mathcal{B}$, this implies that there always exists an optimal solution to (RI) that uses no more than I actions, no matter the cardinality of the menu. For a more general treatment regarding the cardinality of the consideration set in infinite state spaces, see Jung et al. [2019].

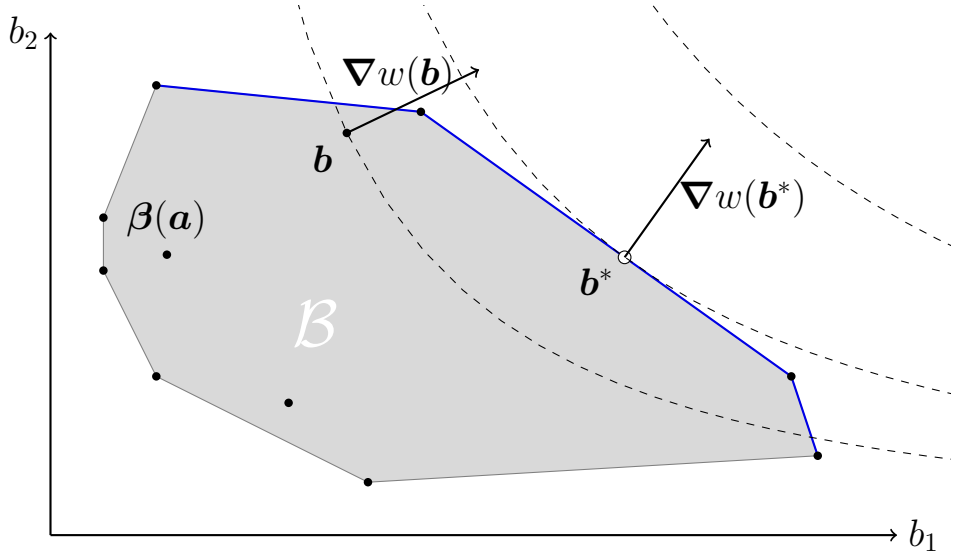

Figure 1: Visual representation of the geometric approach.

vector responds to changes in external parameters.

The weights that describe $\boldsymbol{b}^*$ as a convex combination $\sum_{\boldsymbol{a}\in\mathcal{A}} p(\boldsymbol{a})\boldsymbol{\beta}(\boldsymbol{a})$ over attention vectors indicate the optimal marginals for the original (RI) problem. Conditionals can then be derived by Equation (1). These weights may not be unique, which happens when there are multiple optimal learning strategies in the (RI) problem.

The optimal attention vector can also be of interest by itself. The payoffs from the pre-image $\boldsymbol{\beta}^{-1}(\boldsymbol{b}^*)$ describe a fictitious action that, whether added to the original menu or offered in replacement of it, leaves the decision maker no better or worse off. It is precisely the *ignorance equivalent* of the RI problem, as defined in Müller-Itten et al. [2023], and can play a strategic role in contract games with RI agents.

The spread in the attention vectors that span $\boldsymbol{b}^*$ captures the amount of learning that the decision maker undertakes. This is a consequence of Equation (1), which identifies the optimal conditionals as $P_i(\boldsymbol{a}) = p(\boldsymbol{a})\beta_i(\boldsymbol{a})/b_i^*$. In the extreme case where the optimum is spanned by a single action, $\boldsymbol{b}^* \in \boldsymbol{\beta}(\mathcal{A})$, the decision maker forgoes learning altogether and blindly implements a single action. In all other cases,

the optimal choice involves some learning. Learning is largest when $\boldsymbol{b}^*$ is spanned by wildly different attention vectors, in which case conditionals vary strongly across states, indicating that the agent closely tailors her action to the realized state of the world. The following example with a classic transport theme illustrates the link between the geometric representation and the agent's learning and choice behavior.

Example 1. Bill is choosing a transport option for an upcoming trip. He is familiar with the train route, so this choice yields a certain payoff of zero. Upon consulting the bus map, he sees that there are two bus routes that go to his desired destination: One is direct and yields payoff 0.1, the other includes a long detour and yields payoff -0.9. Unfortunately, Bill is colorblind and cannot tell whether the red or green bus will take the detour. Regardless of trip length, the green bus is a double-decker bus, to which Bill assigns a payoff bonus of 1/3.

We can formalize this as a two-state RI problem, where the red bus takes the detour in state 1 and the green bus in state 2:

$$\boldsymbol{a}^{\mathsf{train}} = \begin{bmatrix} 0 \\ 0 \end{bmatrix}, \quad \boldsymbol{a}^{\mathsf{red\ bus}} = \begin{bmatrix} \text{-}0.9 \\ 0.1 \end{bmatrix}, \quad \boldsymbol{a}^{\mathsf{green\ bus}} = \begin{bmatrix} 0.1{+}1/3 \\ \text{-}0.9{+}1/3 \end{bmatrix}, \text{ and } \boldsymbol{\pi} = \begin{bmatrix} 1/2 \\ 1/2 \end{bmatrix}.$$

In the no-information benchmark where learning the bus colors is impossible ($\lambda \to \infty$), Bill maximizes expected utility and decides to take the train, since $\boldsymbol{\pi} \cdot \boldsymbol{a}^{\mathsf{train}}$ is larger than $\boldsymbol{\pi} \cdot \boldsymbol{a}^x$ for either of the two busses $x \in \{\mathsf{redbus}, \mathsf{greenbus}\}$. Conversely, if learning is free ($\lambda \to 0$), Bill acquires full information and takes the bus with the direct route. Costly learning forms an intermediate scenario where Bill bases his choice on some, but not all, information about the state. Figure 2 illustrates how the attention vectors $\boldsymbol{\beta}(\boldsymbol{a}^x)$ accentuate payoff differences for small information costs λ and attenuate them for large costs.

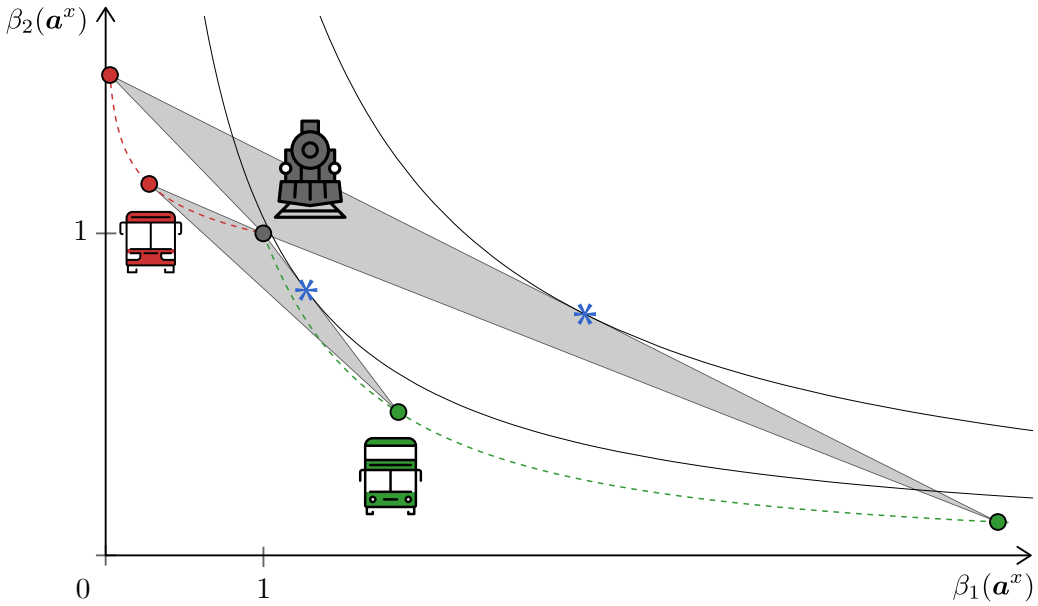

Figure 2: Visual representation of Example 1. As learning becomes more costly ($\lambda \uparrow$), the attention vectors $\boldsymbol{\beta}(\boldsymbol{a}^x)$ of the busses move along the dashed lines, towards that of the train ($\boldsymbol{\beta}(\boldsymbol{a}^{\text{train}}) \equiv \mathbf{1}$ for all λ). Dots indicate their position for cost parameters $\lambda = 0.25$ (top and right) and $\lambda = 0.7$ (closer to origin). In each case, the feasible set $\mathcal{B}$ is drawn in gray and the optimal attention vector is indicated as a blue asterisk. Solid lines represent indifference curves.

When information costs are low ($\lambda = 0.25$), the optimal attention vector is spanned by those of the busses, and Bill never takes the train. But contrary to the full-information solution, he still errs occasionally by taking the detour. We can determine his proclivity for detours by comparing the coordinates along each axis, since Equation (1) pins down the conditional implementation probabilities for each chosen transport option x as $p(\boldsymbol{a}^x)\boldsymbol{\beta}(\boldsymbol{a}^x)/\boldsymbol{b}^*$. As both busses are close to an axis, Bill's error rates are small but not zero: He avoids almost all detours on the red bus, $P_1(\boldsymbol{a}^{\text{red bus}}) \approx 0.04\%$, but accepts some on the green double-decker bus, $P_2(\boldsymbol{a}^{\text{green bus}}) \approx 7.4\%$.

Under moderate information costs ($\lambda = 0.7$), the optimal attention vector is spanned by those of the train and green bus. This indicates that Bill still acquires

some information but also hedges by taking the riskless transport option with probability $p(\boldsymbol{a}^{\mathsf{train}}) \approx 68\%$. As the spread of the attention vectors is smaller, Bill acquires less information. He misses out on many direct green bus trips, $P_1(\boldsymbol{a}^{\mathsf{green\ bus}}) \approx 46\%$, and takes quite a few detours, $P_2(\boldsymbol{a}^{\mathsf{green\ bus}}) \approx 17\%$.

If information costs increase even further, the attention vectors for the busses move closer to that of the train along the dashed lines. As a result, the spread decreases, information acquisition goes down and the error rate goes up, until for some (finite) attention costs he abandons learning altogether and sticks to train rides.

Figure 2 also illustrates how Bill's transport choice changes if he discerns the colors on the map with partial accuracy. If the direct route appears to be painted more green than red, $\pi_1 > \pi_2$, all the indifference curves become steeper but the feasible set $\mathcal{B}$ is left unchanged. For small changes, Bill still uses the same modes of transport, albeit in different contingencies. ◇

3.1 Optimality conditions

The simple structure of (G) allows us to draw upon a vast literature in convex geometry when it comes to locating the optimal attention vector. For instance, the optimal attention vector can be succinctly characterized via linear inequality conditions.

Theorem 1 (Optimality conditions)**.** *The solution $\boldsymbol{b}^* \in \mathcal{B}$ to (G) is unique and fully identified by either of the following two optimality conditions:*

(a) $\nabla w(\boldsymbol{b}^*) \cdot \boldsymbol{\beta}(\boldsymbol{a}) \leq 1$ *for all* $\boldsymbol{a} \in \mathcal{A}$.

(b) $\nabla w(\boldsymbol{b}) \cdot \boldsymbol{b}^* \geq 1$ *for all* $\boldsymbol{b} \in \mathcal{B}$.

Proof. See Appendix A.1. □

Figure 1 captures the geometric intuition for this result: Condition (a) says that $\mathcal{B}$ lies weakly below the hyperplane that is tangent to the indifference curve at $\boldsymbol{b}^*$. Condition (b) says that $\boldsymbol{b}^*$ lies above all hyperplanes that are tangent to the indifference curves at any suboptimal $\boldsymbol{b} \in \mathcal{B}$. Both hold thanks to the convexity of (G).

Both sets of optimality conditions are central to our paper. Constraints (a) are linear over the points in the convex hull $\mathcal{B}$. These constraints have been stated before in terms of action payoffs and form the backbone for Caplin et al. [2018].[5] One key observation is that the conditions jointly imply that the inequality $\boldsymbol{\nabla} w(\boldsymbol{b}^*) \cdot \boldsymbol{b} \leq 1$ binds at the optimal attention vector $\boldsymbol{b} = \boldsymbol{b}^*$. The same must then be true for all attention vectors that span $\boldsymbol{b}^*$, including $\boldsymbol{\beta}(\boldsymbol{a})$ for all actions $\boldsymbol{a}$ that are part of an optimal consideration set.

To our knowledge, the second set of optimality conditions is new to the RI literature. Conditions (b) are constructive in the sense that *any* feasible point $\boldsymbol{b} \in \mathcal{B}$ restricts the potential location of $\boldsymbol{b}^*$ to a linear half-space dictated by the vector $\boldsymbol{\nabla} w(\boldsymbol{b})$. A successive choice of feasible points $\boldsymbol{b}^n \in \mathcal{B}$ then allows us to "close in" on the optimum and make precise statements about the true optimum based on numerical estimates. We lay out how to do so, and the role our novel optimality conditions play, in Section 4.

3.2 Axis Scaling

The functional form of (G) has another separability feature that is particularly helpful for numerical evaluation: Scaling the feasible set $\mathcal{B}$ with a positive constant along any dimension maintains optimality, even if the objective function is left intact. Mathematically, component-wise scaling $\boldsymbol{b} \mapsto [k_i b_i]$ merely offsets the objective value by a

[5] Necessity was highlighted previously by Matějka and McKay [2015].

constant factor,

$$w([k_i b_i]) = \sum_{i \in \mathcal{I}} \pi_i \cdot \ln(k_i b_i) = \boldsymbol{\pi} \cdot \ln(\boldsymbol{b}) + \boldsymbol{\pi} \cdot \ln(\boldsymbol{k}) = w(\boldsymbol{b}) + w(\boldsymbol{k}).$$

As a consequence, the optimum scales by the same vector as the feasible set.

Lemma 1 (Axis Scaling)**.** *Consider any scaling vector* $\boldsymbol{k} \in \mathbb{R}^I_+$*. Attention vector* $\boldsymbol{b}$ *solves (G) if and only if* $[k_i b_i]$ *solves* $\max_{\boldsymbol{b}' \in \{[k_i b_i] \,|\, \boldsymbol{b} \in \mathcal{B}\}} w(\boldsymbol{b}')$*.*

Proof. Since $w([k_i b_i]) = w(\boldsymbol{k}) + w(\boldsymbol{b})$ for all $\boldsymbol{b} \in \mathcal{B}$, $w(\boldsymbol{b}^*) \geq w(\boldsymbol{b})$ for all $\boldsymbol{b} \in \mathcal{B}$ if and only if $w([k_i b_i^*]) \geq w(\boldsymbol{b}')$ for all $\boldsymbol{b}' \in \{[k_i b_i] \,|\, \boldsymbol{b} \in \mathcal{B}\}$. □

Scalability greatly helps reduce floating point imprecision in our numerical algorithm. It also captures the fact that shifting all action payoffs by a constant vector $\boldsymbol{u} \in \mathbb{R}^I$ does not affect the agent's optimal learning strategy — after all, the payoff boost is independent from the action choice.

4 Practical Implications

While there exist powerful algorithms to approximate convex optimization problems like (G),[6] some numerical noise is inevitable. One strength of the geometric approach is that it allows us to narrow down the true optimum based on noisy estimates.

4.1 Consideration set approximations

While agent behavior is ultimately described by the conditional probabilities $\boldsymbol{P}$, there are instances where the primary focus is on identifying which actions are chosen with positive probability. This consideration set reveals which products are on a

[6] We outline one such method in Section 4.3 and compare its effectiveness against other approaches in Section 5.

consumer's radar, predicts possible price jumps in markets with sticky prices, and uncovers correlations in portfolio investments. By classifying some actions as 'never chosen,' it also yields a testable hypothesis for choice data that is too sparse to yield reliable estimates of conditional (or even marginal) implementation probabilities.

We use the optimality conditions from Theorem 1 to approximate the optimal consideration set despite numerical imprecision. To do so, we find it useful to assign scores to each action $\boldsymbol{a} \in \mathcal{A}$ based on any feasible attention vector $\boldsymbol{b} \in \mathcal{B}$. The '$\boldsymbol{b}$-score' of action $\boldsymbol{a}$, written $s(\boldsymbol{a}|\boldsymbol{b}) \in \mathbb{R}$, captures the location of $\boldsymbol{\beta}(\boldsymbol{a})$ relative to the hyperplane tangent to the indifference curve at $\boldsymbol{b}$,

$$s(\boldsymbol{a}|\boldsymbol{b}) := \boldsymbol{\nabla} w(\boldsymbol{b}) \cdot \boldsymbol{\beta}(\boldsymbol{a}) - 1.$$

Actions with positive scores lie above the tangent hyperplane, those with negative scores lie below. Rewriting Theorem 1 in this way, condition (a) states that all actions have non-positive $\boldsymbol{b}^*$-scores, and condition (b) states that the optimal choice has a non-negative expected $\boldsymbol{b}$-score for any $\boldsymbol{b} \in \mathcal{B}$ since

$$\sum_{\boldsymbol{a} \in \mathcal{A}} p(\boldsymbol{a}) s(\boldsymbol{a}|\boldsymbol{b}) = \boldsymbol{\nabla} w(\boldsymbol{b}) \cdot \left[\sum_{\boldsymbol{a} \in \mathcal{A}} p(\boldsymbol{a}) \boldsymbol{\beta}(\boldsymbol{a}) \right] - 1 = \boldsymbol{\nabla} w(\boldsymbol{b}) \cdot \boldsymbol{b}^* - 1 \geq 0. \tag{3}$$

This expression is useful because it allows us to identify the most frequently chosen actions and disregard the rest.

Partial Cover. To account for numeric noise, we generalize the notion of a consideration set to describe any subset of the menu that contains the most frequently chosen actions.

Definition 1. A set $A \subseteq \mathcal{A}$ is a 'q-cover' of the (RI) problem $(\mathcal{A}, \boldsymbol{\pi}, \lambda)$ if and only if

$p(A) = \sum_{\boldsymbol{a} \in A} p(\boldsymbol{a}) \geq q$ for all optimal marginals p.

The consideration set is always a 1-cover, as are any of its supersets. Our goal is to identify q-covers with high probability $q \in [0, 1]$ and small cardinality $|A|$, in order to isolate the most frequently chosen actions.

Starting with any feasible attention vector $\boldsymbol{b}$, Equation (3) implies that the agent can choose actions with negative $\boldsymbol{b}$-scores only if she compensates by often enough choosing actions with sufficiently positive $\boldsymbol{b}$-scores — and when the maximal score $\bar{s}(\boldsymbol{b}) := \max_{\boldsymbol{a} \in \mathcal{A}} s(\boldsymbol{a}|\boldsymbol{b})$ is close to zero, actions with very low scores just cannot be chosen often. This yields a threshold rule that can be used to generate a q-cover for the (unknown) optimal choice based on a numerical approximation.

Corollary 1. *For any $\boldsymbol{b} \in \mathcal{B}$ and any $q \in (0, 1)$, the set*

$$A = \left\{ \boldsymbol{a} \in \mathcal{A} \;\middle|\; s(\boldsymbol{a}|\boldsymbol{b}) \geq -\frac{q\bar{s}(\boldsymbol{b})}{1-q} \right\} \subseteq \mathcal{A}$$

is a q-cover.

Proof. If $\bar{s}(\boldsymbol{b}) = 0$, all $\boldsymbol{b}$-scores are non-positive and the attention vector $\boldsymbol{b}$ is optimal. The set A then contains only actions with a $\boldsymbol{b}$-score of zero, and is equal to the agent's consideration set (or union of consideration sets, if there are multiple optimal solutions). Otherwise, $\bar{s}(\boldsymbol{b}) > 0$ and we proceed by bounding $\boldsymbol{b}$-scores above,

$$\begin{aligned} 0 \overset{(3)}{\leq} \sum_{\boldsymbol{a} \in \mathcal{A}} p(\boldsymbol{a}) s(\boldsymbol{a}|\boldsymbol{b}) &\leq \sum_{\boldsymbol{a} \in \mathcal{A} \setminus A} p(\boldsymbol{a}) \left(-\frac{q\bar{s}(\boldsymbol{b})}{1-q} \right) + \sum_{\boldsymbol{a} \in A} p(\boldsymbol{a}) \bar{s}(\boldsymbol{b}) \\ &= \bar{s}(\boldsymbol{b}) \left[-\frac{q}{1-q}(1 - p(A)) + p(A) \right] = \frac{\bar{s}(\boldsymbol{b})}{1-q} \left[p(A) - q \right] \end{aligned}$$

Dividing by $\bar{s}(\boldsymbol{b})/(1-q)$ yields $p(A) \geq q$. □

Corollary 1 can be readily deployed to assess computation accuracy. Let $\boldsymbol{b}$ be the

researcher's numerical estimate of the optimum and let A be a partial cover with high q, say 95%. The researcher may find that A is pretty large, perhaps close to the full menu $\mathcal{A}$. This may indicate that computational error is substantial if the numerical solution had a small support or, simply, the researcher had reason to expect a sparse consideration set. Alternatively, the researcher may find that A has very few actions or that, from the perspective of the specific application, actions in A are clustered around only a handful of relevant values. In this case, the researcher has effectively identified the key features of the consideration set under the true optimum.

Partial covers are also useful while searching for the right parameters to replicate a salient fact, say, a particular action $\boldsymbol{a}$ being observed with a frequency higher than 10%. The researcher does not need a very precise estimate $\boldsymbol{b}$ of the optimum for each parameter value: As soon as the 90%-cover excludes the aforementioned action $\boldsymbol{a}$, the parameter value can be rejected.

In practice (see Section 5), we find that accurate algorithms yield estimates $\boldsymbol{b}$ that are very close to the (G) solution. The resulting q-covers typically have small cardinality even when q is close to one, making this approach very attractive for empirical research.

Dominated Actions. In many situations, it is even possible to rule out some dominated actions altogether — effectively finding a 1-cover that is significantly smaller than the menu. Sometimes, this is trivial: If an action delivers less payoff in each state than a blind lottery over other actions, the action is suboptimal at any posterior and thus would never be chosen. Tighter bounds are possible, since the optimality conditions (a) and (b) imply that any action in the consideration set has a $\boldsymbol{b}^*$-score of zero. Using numerical approximations, it is often possible to limit the location of the possible optimal attention vector $\boldsymbol{b}^*$, which in turn restricts the possible gradient

$\nabla w(\boldsymbol{b}^*) = [b_i/\pi_i]$ to some subset $\Psi \subset \mathbb{R}^I_+$. If we can bound the feasible $\boldsymbol{b}^*$-scores for some action $\boldsymbol{a}$ below zero,

$$s(\boldsymbol{a}|\boldsymbol{b}^*) \leq \sup_{\boldsymbol{\psi}\in\Psi} \boldsymbol{\psi} \cdot \boldsymbol{\beta}(\boldsymbol{a}) - 1 < 0, \tag{4}$$

we can rule it out for good. The RI agent never implements this action in an optimal solution.

Computationally, finding dominated actions is significantly slower than finding a partial cover. A valid q-cover can be obtained from any feasible attention vector based solely on explicit score computations, while testing for dominance requires determining first a feasible set of gradients Ψ, and then solving maximization problem (4) for each individual action. Still, the dominated actions approach is useful in situations where accuracy is paramount.

4.2 Precision Metric

Even though (G) is computationally simpler, the primary object of interest is ultimately the conditional choice P that predicts behavior, not the optimal attention vector. Be it to compare model predictions to empirical data, or to write a stopping criterion for numerical methods, the researcher eventually needs to decide when two conditional choices are "similar." We now show that the distance between implied attention vectors offers a parsimonious metric to gauge similarity of the implied conditional choice.

Definition 2. The *attention distance* between choices $\boldsymbol{P}, \boldsymbol{P}' \in (\Delta\mathcal{A})^I$ is defined as

$$d_{(\mathrm{G})}(\boldsymbol{P}, \boldsymbol{P}') := \sqrt{\sum_{i\in\mathcal{I}} \pi_i \left(\beta_i^{-1}\big(\mathsf{E}[\beta_i(\boldsymbol{a})|\boldsymbol{a}\sim P_i]\big) - \beta_i^{-1}\big(\mathsf{E}[\beta_i(\boldsymbol{a})|\boldsymbol{a}\sim P_i']\big)\right)^2}.$$

The attention distance is obtained in three steps: First, we compute the expected attention vector $[\mathsf{E}[\beta_i(\boldsymbol{a})|\boldsymbol{a} \sim P_i]]$ under each conditional $\boldsymbol{P}$. Then, we transform the attention vector back into the original payoff space using the inverse mapping $\boldsymbol{\beta}^{-1}$. This transformation gets rid of any distortions introduced by axis scaling. Finally, we apply the standard Euclidean metric to the resulting payoff vectors, weighted by the prior probability for each state. The weights ensure that the distance is unaffected by a payoff-irrelevant splitting of states. Nonnegativity, symmetry, and the triangle inequality are directly inherited from the standard Euclidean distance.

A potential shortcoming of the attention distance is its failure to distinguish between choices that imply the same attention vector: From a computational perspective, this may be a satisfactory compromise in the interest of parsimony. Indeed, we now show that distance $d_{(\mathrm{G})}$ provides a suitable convergence criterion whenever (RI) admits a unique solution: From any sequence of conditionals $\boldsymbol{P}^n$ that converge to the solution $\boldsymbol{P}$ under $d_{(\mathrm{G})}$, we can construct conditionals that converge in terms of both marginal and conditional probabilities. So although the attention distance only considers I-dimensional vectors, it is sufficient to generate convergence for all $I \times |\mathcal{A}|$ conditional probabilities thanks to continuity of the first-order conditions in Equation (1).

Lemma 2. *Suppose (RI) admits a unique solution $\boldsymbol{P}$. For any sequence of conditionals $\{\boldsymbol{P}^n\} \subset (\Delta\mathcal{A})^I$ that converges to $\boldsymbol{P}$ according to $d_{(G)}$, the conditionals*

$$\left[\frac{(\boldsymbol{\pi} \cdot \boldsymbol{P}^n(\boldsymbol{a}))\beta_i(\boldsymbol{a})}{\sum_{\boldsymbol{a}' \in \mathcal{A}}(\boldsymbol{\pi} \cdot \boldsymbol{P}^n(\boldsymbol{a}'))\beta_i(\boldsymbol{a}')}\right] \tag{5}$$

converge to $\boldsymbol{P}$ under the standard Euclidean metric over $(\Delta\mathcal{A})^I$.

Proof. See Appendix A.1. □

The attention distance $d_{(\mathrm{G})}$ is ideally suited to serve as a stopping criterion for numerical solution methods since it penalizes numerical noise when it leads to substantial payoff differences and ensures that conditional choices converge to the actual optimum. In this sense, the attention distance strikes a balance between other common stopping criteria: Methods that rely on objective values alone can lead to noisy estimates of the model's behavioral implications, since several conditional choices may — and often do [Jung et al., 2019] — share very similar objective values. At the other end, a straightforward comparison based on the Euclidean distance between the conditional matrices $\boldsymbol{P}$ and $\boldsymbol{P}'$ (or the vectors of marginals p and p') treats all actions as equally distinct. However, numerical (RI) estimates over large menus err along both the extensive and intensive margin: They typically misidentify both the support of the optimal choice (the consideration set) as well as the relative frequency of chosen actions. The matrix distance disproportionately penalizes errors on the extensive margin, while $d_{(\mathrm{G})}$ recognizes when a candidate consideration set contains near-optimal actions.

4.3 Algorithm Design

The simple geometry of (G) offers fertile ground for numerical methods that solve finite RI problems. Standard algorithmic techniques for convex problems perform well, and the reduced dimensionality of (G) brings obvious gains in performance.

We provide an algorithm based on Sequential Quadratic Programming (SQP) and active set methods (see, e.g. Judd [1998]), using $d_{(\mathrm{G})}$ as a stopping criterion. We refer to this algorithm as *GAP-SQP*, where 'GAP' stands for *Geometric Attention Problem*. The codes are available at `https://github.com/mmulleri/GAP-SQP` and a detailed explanation of the code is provided in Appendix A.2. Although the optimization

methods we use are relatively unsophisticated, we find that our algorithm performs favorably when compared to other state-of-the-art techniques that are typically used to estimate RI models, in terms of both speed and accuracy. The methods and ideas can also be combined with other solution methods to yield further gains in performance.[7]

A few practical challenges arise when dealing with large state and action spaces, for example when approximating continuous RI problems. This can routinely lead to memory issues when storing and accessing the payoff matrix,[8] and we briefly elaborate on them here.

Dealing with large menus. Large menus can often be partitioned into clusters of actions with similar payoff vectors. Sometimes, this clustering is explicit since the menu represents a discrete approximation to a continuous choice variable, and so the granularity of the discretization grid determines which actions are 'lumped together'. Even if the goal is to characterize the optimal choice over a very fine grid, active set methods can significantly speed up the algorithm and reduce memory usage.

Practically, we start with a coarse grid over actions and increase the grid precision stepwise. At each step, we compute the optimal attention vector $\boldsymbol{b}^k$ and then include K actions from the finer grid with the highest $\boldsymbol{b}^k$-score $s(\boldsymbol{a}|\boldsymbol{b}^k)$. We increase grid precision once the 99% cover stabilizes. When K is large relative to the optimal consideration set, this approach can approximate large action spaces without running into memory management issues. And while the numerical estimates of the algorithm depend on the path of subgrids, any partial covers computed in the last round accurately describe the optimal choice over the *entire* menu $\mathcal{A}$.

[7] Such as replacing the SQP approach with more advanced convex optimization algorithms.

[8] In the portfolio optimization (Section 5.2) the associated $300^2 \times 300^2$ payoff matrix would require 64.8Gb of memory.

Large state spaces. Although this step-wise optimization effectively avoids the load of large menus, each step still relies on the entire payoff vectors for the currently considered actions. As such, large state spaces inherently pose a bigger challenge for our algorithm than large menus. When memory constraints are binding, a lower threshold K may offer some relief: By reducing the number of actions that are added to the candidate consideration set at each step, fewer payoff vectors are considered simultaneously, but more iterations may be necessary to achieve convergence.

Approximating continuous problems. Learning generates payoff complementarities across actions [Müller-Itten et al., 2023]. When using discrete approximations to continuous problems, it is thus possible that even a fine grid $\mathcal{A} \times \mathcal{I}$ over actions and states fails to capture the full learning opportunities, and that any approximation thus dismisses some actions in error. That said, it appears in practice that the geometric approach also provides sensible numerical estimates when applied to a fine discretization of a continuous (RI) problem, as we show in the applications below.

Solving dynamic problems. When the agent faces repeated decisions and the underlying state is autocorrelated across time, learning yields actionable information about both the present and the future. The continuation value of learning is endogenous, but typically increases the agent's incentives to learn.

Although our approach is static in nature, it can easily be incorporated into iterative algorithms that account for these dynamic incentives, such as the one proposed by Miao and Xing [2022] for situations with unobservable payoffs. They express the agent's problem at any history as a static problem with payoffs given by appropriately constructed value vectors, then approximate the agent's optimal learning strategy using an iteration of the Blahut-Arimoto algorithm, and in turn use these strategies

to update the associated (Markovian) beliefs and continuation values. We simply replace the Blahut-Arimoto step with our GAP-SQP algorithm, and find notable speed gains — driven by the fact that beliefs and actions converge in far fewer iterations.[9]

5 Applications

In this section, we illustrate by way of example that both the conceptual framework and the computationally tractable algorithm have the potential to expand the purview of further research. We consider two applications: The first is a monopolist problem with uncertain demand as proposed by Matějka [2016]. We use this well-known application to benchmark the GAP-SQP algorithm described in Section 4.3 against existing methods, focusing primarily on speed. We then extend this model to multiple interconnected periods to highlight how our algorithm can be combined with the iterative approach of Miao and Xing [2022] to tackle dynamic RI problems.

The second is a portfolio choice problem with a massive state and action space proposed by Jung et al. [2019]. We primarily use it to highlight the precision of GAP-SQP and showcase the robust behavioral predictions that we develop in Section 4.1.

5.1 Sticky Prices [Matějka, 2016]

Our first application is based on the 'rationally inattentive seller' model of Matějka [2016]. A monopolistic seller has a per unit input cost of 1 and sets the price p facing an isoelastic demand function with elasticity $\frac{d+1}{d}$. The elasticity parameter d is uniformly distributed over the interval $\left[\frac{1}{9}, \frac{1}{2}\right]$, and the seller can learn its value through costly learning. Profits are given by $\Pi(d, p) = p^{-\frac{d+1}{d}}(p-1)$, with d describing

[9] A detailed description of our dynamic algorithm can be found in Appendix A.2.2.

the state of the world and p the seller's action.[10] As in Matějka [2016], actions and states are discretized.

For comparison with our base routine described in Section 4.3, we also solve the model using the Blahut-Arimoto (BA) algorithm, a solution method that originated in Rate Distortion theory and has recently gained some usage in RI problems. The BA algorithm iterates between candidate marginal and conditional distributions[11] and, like GAP-SQP, is guaranteed to converge to the optimum.[12]

Figure 3 documents the running times in seconds across a range of information costs λ for our benchmark case with a grid of 200×200 points. As shown in panel (a), the GAP-SQP algorithm terminates in less than 0.05 seconds in all runs, with minimal differences across information costs. The BA algorithm, reported in panel (b), runs in about one second when information costs are very low — and thus the solution is very close to the full information benchmark — but is substantially slower for higher information costs, up to 20 seconds. Both algorithms achieve very similar objective values, with the GAP-SQP algorithm outperforming by about 10^{-8}.[13]

The reason why GAP-SQP outperforms the BA algorithm is twofold. First, wide swaths of potential actions (prices) are dominated in this example. The GAP-SQP quickly drops them from consideration, which drastically reduces the size of the prob-

[10] Matějka [2016] assumes a channel capacity constraint rather than information being acquired at a cost. To match the channel capacity constraint of half a bit, we find that we need to set $\lambda = 5.31 \times 10^{-3}$.

[11] Given any candidate marginals p, the BA algorithm obtains candidate conditionals P using Equation (1), and then uses the law of total probabilities, $p(\boldsymbol{a}) = \boldsymbol{\pi} \cdot \boldsymbol{P}(\boldsymbol{a})$, to update its guess for p.

[12] We implement both algorithms in MATLAB, using an iMac desktop computer with 24 GB of RAM and an 3.4 GHz Quad-Core Intel Core i5 processor. For further discussion of the BA algorithm, see Caplin et al. [2018] and Cover and Thomas [2012]. Matějka [2016] instead used proprietary software AMPL/LOQO to solve for the joint probability distribution. Due to licensing restrictions, we were not able to use AMPL/LOQO to document running times. A comparable, freely available solver (IPOPT) was substantially slower and less precise than both the GAP-SQP and BA algorithms.

[13] Numerical solutions for $\lambda = 5.31 \times 10^{-3}$ are also very similar to those reported in Matějka [2016]. See online Appendix B.1. We thank Filip Matějka for sharing his numerical output.

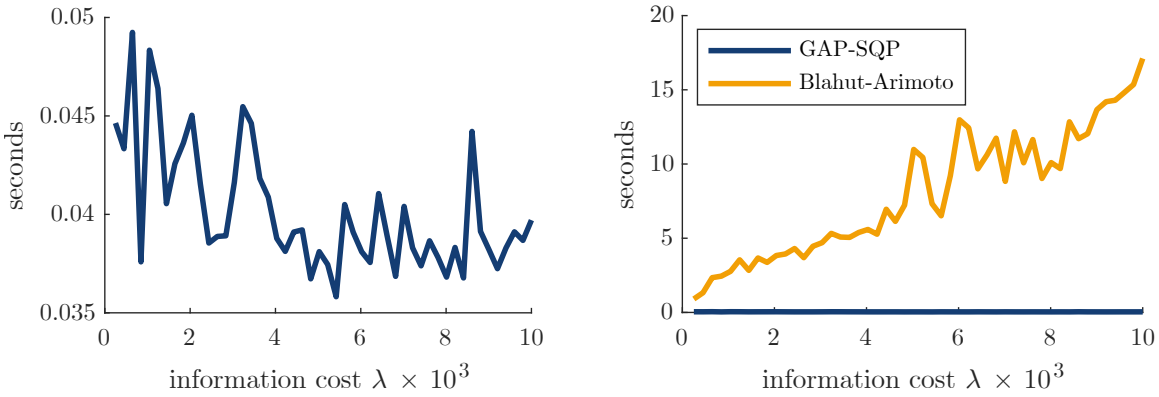

(a) GAP-SQP algorithm

(b) Algorithm comparison

Figure 3: Running times across information costs

lem in later iterations. BA never drops actions, and must continue to construct conditional and marginal probabilities over each and every one until the algorithm converges. This turns out to be a computationally slow process, despite its simplicity.

The second reason is that the BA algorithm is an iterative procedure whose convergence speed is determined by the information cost: The lower the information cost, the faster the convergence rate. As a result, higher information costs converge more slowly and require more iterations, which translates to longer solution times.

While our GAP-SQP algorithm is also sequential, its convergence speed is not directly affected by the information cost. The information cost serves only to construct the convex constraint set over which the GAP-SQP optimizes in each iteration. It is not surprising, therefore, that Figure 3(a) reveals very little correlation between information cost and solution time for the GAP-SQP. For this reason, our algorithm is particularly appealing at higher information costs.

Next we ratchet up the computation burden by increasing each grid precision up to 600 points, adding up to $600^2 = 360,000$ total grid points. As shown in Figure 4(a), running times scale roughly linearly for the GAP-SQP algorithm. Even at a 600×600 grid running times stay well below half a second. Figure 4(b) shows that

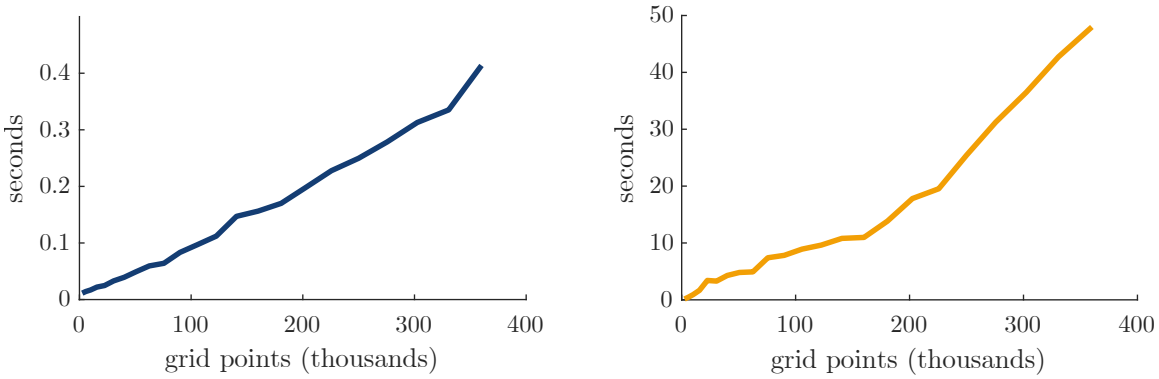

(a) GAP-SQP algorithm

(b) Blahut-Arimoto algorithm

Figure 4: Running times across grid precision

the BA algorithm also scales well; though this means that computing times approach a minute for the largest grids.

We also compute the set of undominated actions as well as the 99% cover using the output from our GAP-SQP algorithm. Figure 5 displays the GAP-SQP numerical solution as solid bars over the full price grid — with insets at two points of the full support of prices for visibility. The 99% cover is indicated with a dark blue background. It is identical to the consideration set of the numerical solution. Thus, even if we had low confidence in the accuracy of the numerical estimate, we would be able to conclude that the total probability of observing any price outside of this set is at most 1%. Indeed, the main point in [Matějka, 2016] is that optimal pricing behavior is discrete, clustering mass on a comparatively small number of points. This observation can also be made by looking at the set of undominated actions (light blue background): It shows that the vast majority of prices are not used in any contingency. The validity of the claim does not rely on having found the true optimum of the (RI) problem, which makes it significantly more robust.

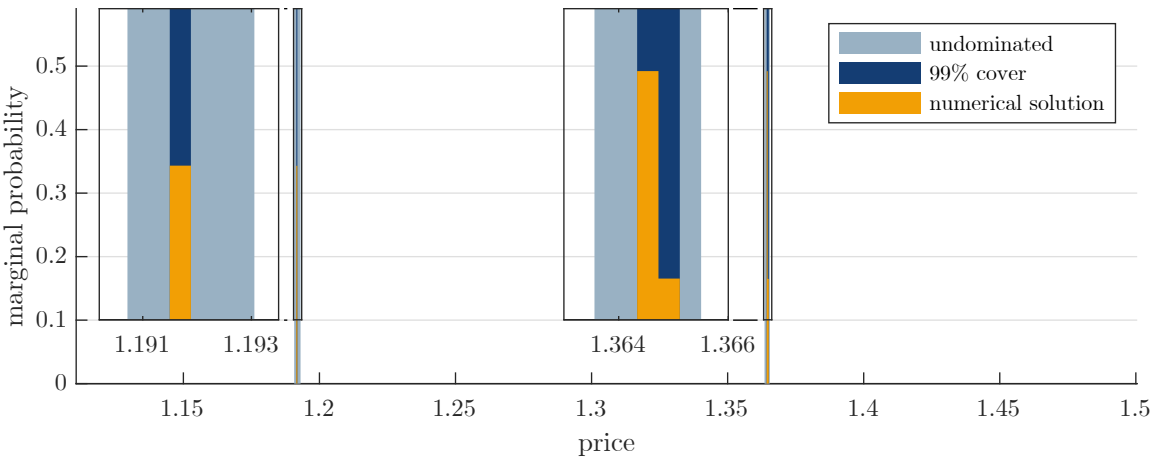

Figure 5: Partial cover and undominated actions, with 300 states and 1000 actions.

Dynamic Extension. To assess the promise of our approach for dynamic applications, we extend the model in [Matějka, 2016] to multiple periods with the elasticity parameter following a discretized AR(1) process. Formally, we let $d_t = (1-\rho)\bar{d} + \rho d_{t-1} + \varepsilon_t$ where $\bar{d} = \frac{11}{36}$ is the average elasticity, ε_t follows a mean-zero normal distribution and $\rho = 0.7$ governs the autocorrelation. The variance of ε_t is chosen so that the state range $[\frac{1}{9}, \frac{1}{2}]$ extends three standard deviations to either side of the mean under the unconditional distribution (as in Tauchen [1986]). As before, the agent sets the price $p_t \in [\frac{10}{9}, \frac{3}{2}]$ and enjoys flow payoff $\Pi(d_t, p_t)$.[14] For simplicity, we assume that there is no discounting and maintain the same information cost parameter as before.

We discretize the action and state spaces with 100 and 300 grid points, respectively, and consider a time horizon of $T = 10$ periods, resulting in 901 interconnected RI problems.[15] We implement the iterative algorithm suggested by Miao and Xing

[14] As in Miao and Xing [2022], we assume that the agent cannot learn 'for free' simply by observing past payoff realizations.

[15] The full solution specifies the agent's initial choice, as well as her continuation strategy after each of 100 Markov histories p_{t-1} during each of the subsequent time periods. Choices in future periods affect the continuation values that guide the agent's earlier choices, and choices in earlier periods inform the agent's subsequent beliefs.

[2022] using either the Blahut-Arimoto or the GAP-SQP subroutine to update strategies. Figure 6(a) plots the welfare that is achieved by the algorithmic solutions after different running times.[16] Although each iteration takes more time with GAP-SQP than with BA (6 rather than .5 seconds on average), the algorithm converges in significantly fewer iterations. When compared over the same running time, GAP-SQP achieves higher expected welfare than the BA variant. The faster convergence can also be seen when we compute sufficiency scores in panel (b), as in Section 4.1. We plot the maximal score $\bar{s}$ across all actions in any subgame, knowing that it should be zero under the optimal choice. It takes four iterations (26 seconds) for the GAP scores to drop below those of the BA variant, after which they quickly approach zero while the BA scores taper out at a higher level.[17] At the end of our evaluation period, $\bar{s}$ settles below 10^{-5} under GAP-SQP, while the score converges to about 0.05 under BA after 300 seconds. Since the threshold score for inclusion in the partial covers is proportional to $\bar{s}$ (Corollary 1), this 5000-fold improvement suggests that not only does the solution from the geometric approach yield a strategy that outperforms BA, it also much more tightly identifies the optimal behavior.

5.2 Portfolio Choice [Jung et al., 2019]

Our second application considers the portfolio choice problem of Jung et al. [2019], who illustrate that RI can explain low rates of household portfolio rebalancing. In this problem, an investor with unit wealth designs a portfolio composed of three uncorrelated assets, without restrictions on short sales or overall leverage. The investor has constant absolute risk aversion (CARA) utility $u(x) = -e^{-\alpha x}$ with risk aversion

[16] All benchmark operations are carried out on a 2021 iMac with 16GB of RAM and a Apple M1 Processor.

[17] While the BA algorithm is known to be welfare monotonic, not every component of the solution improves over time. Figure 6(b) shows such a nonmonotonicity in the maximal sufficiency score $\bar{s}$.

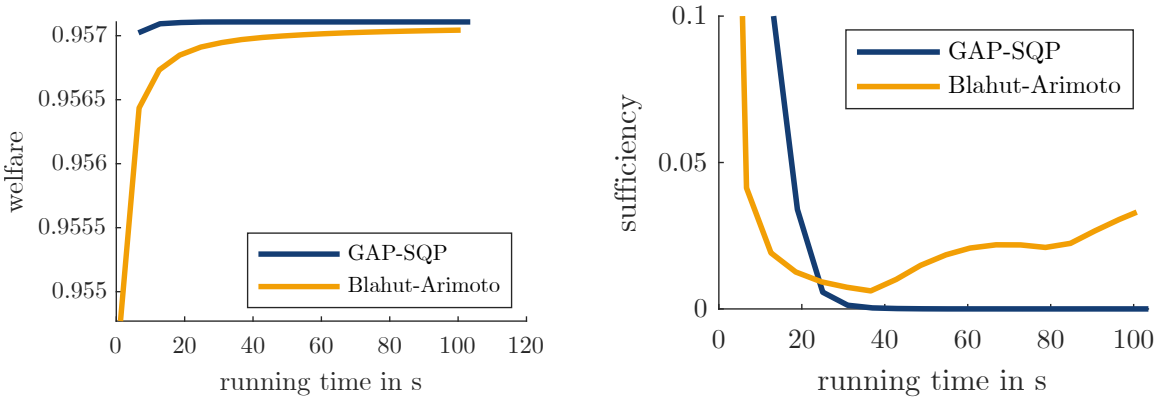

(a) achieved welfare

(b) sufficiency score

Figure 6: Comparison of the numerical solution at different running times

parameter α. Asset zero is a safe asset with constant return 1.03. The returns from risky assets $j = 1$ and $j = 2$ are each modeled as the sum of two independent random variables around a slightly higher mean return, $1.04 + Z_j + Y_j$. The random variable $Z_j \overset{\text{iid}}{\sim} \mathcal{N}(0, \sigma_z^2)$ reflects factors that are inherently unforeseeable. The random variable Y_j reflects factors that are not known at the outset but can be learned at a cost. Each portfolio $(\theta_1, \theta_2) \in \mathbb{R}^2$ describes an available action, where θ_j is the position in risky asset j and $\theta_0 := 1 - \theta_1 - \theta_2$ is the position in the safe asset. The expected utility from the portfolio conditional on state $\boldsymbol{Y} = (Y_1, Y_2)$ is

$$U(\boldsymbol{\theta}, \boldsymbol{Y}) = \mathsf{E}\left[u\left(1.03\theta_0 + \sum_{j=1}^{2} (1.04 + Z_j + Y_j)\theta_j \right) \middle| \boldsymbol{Y} \right]. \tag{6}$$

We follow Jung et al. [2019] and assume that $\boldsymbol{Y}$ follows a discrete distribution over a 300×300 grid that is obtained from a normal distribution $\mathcal{N}(\mathbf{0}, 0.02^2 I)$ truncated at three standard deviations. We report results for parameter values $\alpha = 1$, $\lambda = 0.1$, and $\sigma_z = 0.0173$.[18]

[18]These parameters correspond to scenario B in Jung et al. [2019]. Although we show results only for this scenario, the GAP-SQP solution has larger support and achieves a higher objective value than the JKMS solution in all four parameter scenarios.

We approximate the continuous menu $(\theta_1, \theta_2) \in \mathbb{R}^2$ by first (without loss of generality) imposing the upper and lower bounds given by the full-information solution, and then iteratively doubling the grid resolution using 99.99% covers until we reach $513 \times 513 = (2^9 + 1)^2$ points.[19] Jung et al. [2019] instead use a variant of the Blahut-Arimoto algorithm that optimizes the points of support at each step of the algorithm. We refer to this algorithm as JKMS. The algorithms reach a comparable objective value, with GAP-SQP mildly outperforming JKMS. Both algorithms perform significantly better than the optimal multivariate Gaussian solution,[20] an approach that is common in the applied literature.[21]

Turning to the behavioral implications, Figure 7(a) shows the estimated portfolio choice probabilities across all three algorithms. The Gaussian solution stands out as the only continuous solution, but even the two discrete solutions are measurably different. Jung et al. [2019] caution that their solution method may miss solutions with a larger support, and this is exactly what we find with GAP-SQP. The main point in Jung et al. [2019], that portfolio rebalancing is relatively rare, remains valid — and indeed the consideration set shrinks for higher information costs. Quantitatively, though, GAP-SQP finds that portfolio rebalancing is substantially more common and, occasionally, the investor makes small adjustments.

[19] The iterative approach (see Section 4.3 and Appendix A.2) allows us to handle a large action grid. However, it does not reduce the memory demands imposed by the large state space. In order to compute the solution at the same state grid resolution as Jung et al. [2019], we opted to run the algorithm on a computational cluster.

[20] The solution published in Jung et al. [2019] closes 0.225 of the payoff gap between no and free information (corresponding to $\lambda \to \infty$ and $\lambda \to 0$ respectively), while GAP-SQP closes 0.238 of the gap. The best Gaussian solution closes roughly 0.112 of the payoff gap. For details on the best Gaussian solution and a comparison of statewise payoff distributions across algorithms, see Online Appendix B.2.

[21] Many papers assume a Gaussian signal structure as a primitive for tractability [Kacperczyk et al., 2016, Luo et al., 2017, Mondria, 2010, Van Nieuwerburgh and Veldkamp, 2009, 2010]. Others [Maćkowiak and Wiederholt, 2009, 2012] use a quadratic approximation to the objective function, which implies a Gaussian signal at the optimum given a Gaussian state. In our case, the quadratic approximation reaches lower welfare than the no-information solution, so we compare against the optimal Gaussian CARA solution.

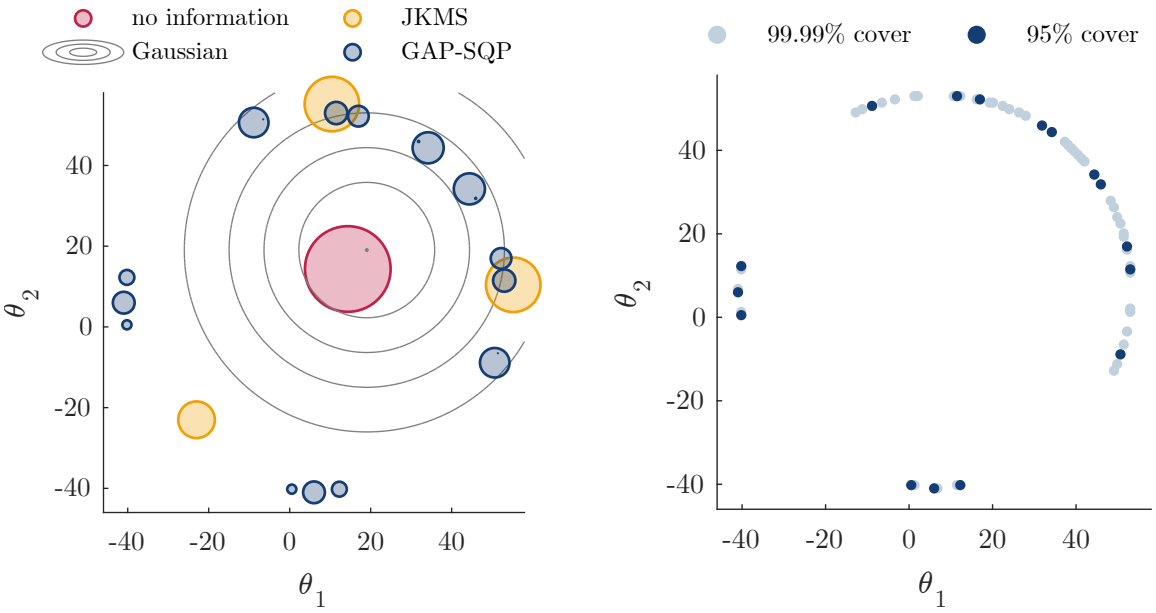

(a) estimated portfolio choice

(b) partial covers

Figure 7: Portfolio distributions under GAP-SQP (blue), JMKS (orange), and optimal Gaussian (gray), as well as the information benchmark (red). In panel (a), the circle size of each portfolio $\boldsymbol{\theta}$ is proportional to the probability weight $p(\boldsymbol{\theta})$, and the probability that the Gaussian solution falls between any two contour lines is equal to 0.2. In panel (b), the circle size is fixed and each portfolio in the 95% cover (dark blue) is also in the 99.99% cover (light blue).

The partial covers displayed in Figure 7(b) allow more robust statements regarding the true optimum given the state and action grid that we use. Contrary to the JKMS estimates, it appears that the investor almost never takes short positions simultaneously on both risky assets, $\boldsymbol{\theta} \ll \mathbf{0}$. This may suggest that the investor looks for good news rather than bad. Another pattern that arises from Figure 7(b) is that the RI investor selects only portfolios from a circle, hinting that some further analytic results are possible, which may help elucidate the relative role of risk aversion and information processing costs, for instance.[22] Overall, the example illustrates the need for more robust estimation techniques that not only deliver a 'better' estimate but allow a valid characterization of the true optimal choice.

[22] A more thorough investigation of this conjecture is outside the scope of this research.

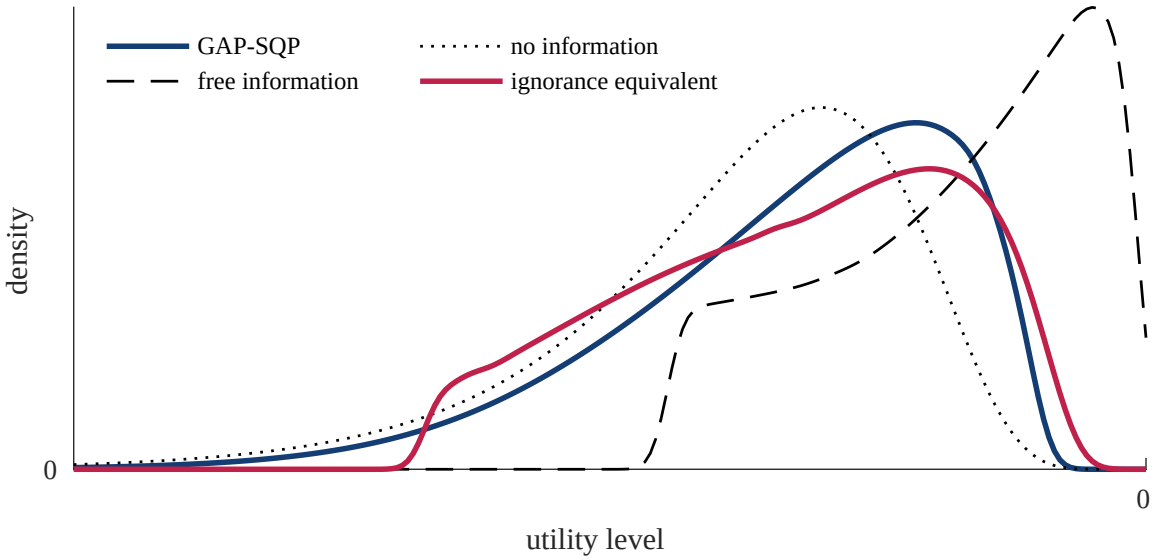

Figure 8: Payoff distribution across choices, smoothed with a kernel density estimate with bandwidth 0.01.

Figure 8 plots the statewise payoff distribution $U(\boldsymbol{\theta}, \boldsymbol{Y}) - \lambda \mathsf{MI}$, assuming $(\boldsymbol{\theta}, \boldsymbol{Y})$ is distributed according to the numeric solution of GAP-SQP (blue) and the information cost MI is borne unconditionally. For comparison, we also show the payoff distribution under no information ($\lambda \to \infty$, grey dotted) and free information ($\lambda \to 0$, grey dashed).

We can compute the ignorance equivalent of this RI investment problem, obtained as the pre-image $\boldsymbol{\beta}^{-1}(\boldsymbol{b}^*)$ of the optimal attention vector. This fictitious asset is uniquely designed to ensure that the investor would abandon learning and select it unconditionally, but without gaining a payoff boost in doing so [Müller-Itten et al., 2023]. The ignorance equivalent yields the same expected utility as the optimal portfolio choice with learning, but – as can be seen from the payoff distribution in Figure 8 – it avoids the lowest payoffs to dissuade learning. In that way, it mimics the full-information distribution.

6 Conclusion

We have introduced a novel geometric approach to finite RI models and developed a computational toolkit with a focus on robust methods for behavioral predictions. Our hope is that our contribution enables further substantial progress in more complex, quantitatively-relevant RI models — the kind necessary for applied work.

We conclude with some observations regarding RI models with a continuum of actions or states. These are commonplace in macroeconomics and finance, where researchers typically either focus on specific functional forms that can be solved analytically or approximate the solution with a tractable distribution. Our methods provide both an alternative and a complement to these distributional assumptions through discretization of the action and state spaces. Given our computational gains, it is possible to use very fine grids to minimize precision loss. Researchers can thus now assess how general the analytic functional forms are or whether distributional approximations are satisfactory. If the behavioral implications prove to be robust, then the elegance and tractability of the analytic or approximate solutions justify their use. If they do not, then discretization may be preferable — with the advantage that it grants the researcher more flexibility in tailoring the payoffs and beliefs to data.

A Appendix

A.1 Additional Proofs

We start by showing that it is without loss of generality possible to relax the (RI) optimization such that the decision maker can separately choose the marginals $p \in \Delta\mathcal{A}$ and conditionals $\boldsymbol{P} \in (\Delta\mathcal{A})^I$,

$$\max_{p \in \Delta\mathcal{A}, \boldsymbol{P} \in (\Delta\mathcal{A})^I} \sum_{i \in \mathcal{I}} \pi_i \left[\sum_{\boldsymbol{a} \in \mathcal{A}} P_i(\boldsymbol{a}) a_i - \lambda D_{\mathsf{KL}}(P_i \,\|\, p) \right], \tag{7}$$

where $D_{\mathsf{KL}}(P_i \,\|\, p) = \sum_{\boldsymbol{a} \in A} P_i(\boldsymbol{a}) \ln\left(\frac{P_i(\boldsymbol{a})}{p(\boldsymbol{a})}\right)$ denotes the Kullback-Leibler divergence between P_i and p.

Lemma 3. *The optimal conditionals $\boldsymbol{P}$ in (RI) and the relaxed problem Equation (7) are equal, and the optimal marginals in Equation (7) satisfy $p(\boldsymbol{a}) = \boldsymbol{\pi} \cdot \boldsymbol{P}(\boldsymbol{a})$ for all $\boldsymbol{a} \in \mathcal{A}$.*

Proof. It is an exercise in pure algebra to show that

$$\begin{aligned}
&\sum_{i \in \mathcal{I}} \pi_i \left[D_{\mathsf{KL}}(P_i \,\|\, p) - D_{\mathsf{KL}}(P_i \,\|\, \boldsymbol{\pi} \cdot \boldsymbol{P}) \right] \\
&\qquad = \sum_{i \in \mathcal{I}} \pi_i \sum_{\boldsymbol{a} \in \mathcal{A}} P_i(\boldsymbol{a}) \left[\ln(P_i(\boldsymbol{a})) - \ln(p(\boldsymbol{a})) - \ln(P_i(\boldsymbol{a})) + \ln(\boldsymbol{\pi} \cdot \boldsymbol{P}(\boldsymbol{a})) \right] \\
&\qquad = \sum_{\boldsymbol{a} \in A} \boldsymbol{\pi} \cdot \boldsymbol{P}(\boldsymbol{a}) \left(\ln(\boldsymbol{\pi} \cdot \boldsymbol{P}(\boldsymbol{a})) - \ln p(\boldsymbol{a}) \right) = D_{\mathsf{KL}}(\boldsymbol{\pi} \cdot \boldsymbol{P} \,\|\, p) \geq 0,
\end{aligned}$$

with strict inequality whenever $p(\boldsymbol{a})$ differs from $\boldsymbol{P}$'s marginals $\boldsymbol{\pi} \cdot \boldsymbol{P}(\boldsymbol{a})$. Consequently, any other choice of p would increase costs without any consumption benefits. By optimality, the agent avoids all unnecessary costs by setting $p = \boldsymbol{\pi} \cdot \boldsymbol{P}$. □

Next, we formally establish the validity of the optimality conditions that are

central to our results.

Proof of Theorem 1: Since w is strictly concave over a compact domain $\mathcal{B}$, it admits a unique maximum. We first show that the optimum $\boldsymbol{b}^*$ necessarily satisfies both conditions. Indeed, consider any $\boldsymbol{b} \in \mathcal{B} \setminus \{\boldsymbol{b}^*\}$ and let $\boldsymbol{\eta} : [0,1] \to \mathcal{B}$ be defined as $\boldsymbol{\eta}(t) = t\boldsymbol{b}^* + (1-t)\boldsymbol{b}$. The function $w \circ \boldsymbol{\eta}$ represents the gain in utility as the attention vector moves from $\boldsymbol{b}$ towards $\boldsymbol{b}^*$. The function is strictly increasing: If $t < t'$, then

$$(w \circ \boldsymbol{\eta})(t') > \frac{t'-t}{1-t} w(\boldsymbol{\eta}(1)) + \frac{1-t'}{1-t} w(\boldsymbol{\eta}(t)) \geq (w \circ \boldsymbol{\eta})(t),$$

where the first inequality follows from strict concavity of w and the second from optimality of $\boldsymbol{b}^*$, as $w(\boldsymbol{\eta}(1)) = w(\boldsymbol{b}^*) \geq w(\boldsymbol{\eta}(t))$. Since the derivative of $(w \circ \boldsymbol{\eta})$ is equal to $\boldsymbol{\nabla} w(\boldsymbol{\eta}(t)) \cdot (\boldsymbol{b}^* - \boldsymbol{b})$, and $\boldsymbol{\nabla} w(\boldsymbol{b}) \cdot \boldsymbol{b} = \sum_{i \in \mathcal{I}} \lambda \frac{\pi_i}{b_i} b_i \equiv 1$ by construction, the nonnegativity of $(w \circ \boldsymbol{\eta})'(1)$ yields condition (a) and the nonnegativity of $(w \circ \boldsymbol{\eta})'(0)$ yields (b).

We show sufficiency through the contrapositive: If $\boldsymbol{b}^*$ is not optimal, then it satisfies neither condition. Let $\boldsymbol{b}$ equal the true optimum and define $\boldsymbol{\eta}(t)$ as above. The function $(w \circ \boldsymbol{\eta})$ is now strictly decreasing since $w(\boldsymbol{\eta}(0)) > w(\boldsymbol{\eta}(t'))$ by uniqueness of the optimum and hence for any $t < t'$,

$$(w \circ \boldsymbol{\eta})(t) \geq \frac{t'-t}{t'} w(\boldsymbol{\eta}(0)) + \frac{t}{t'} w(\boldsymbol{\eta}(t')) > (w \circ \boldsymbol{\eta})(t').$$

At $t = 1$, the condition $(w \circ \boldsymbol{\eta})'(t) < 0$ violates (a) and at $t = 0$ it violates (b). □

Proof of Lemma 2: Consider any subsequence $\{\boldsymbol{P}^{n_k}\}$ that converges to some conditionals $\bar{\boldsymbol{P}}$ under the standard Euclidean metric over $(\Delta\mathcal{A})^{\mathcal{I}}$. Since $\boldsymbol{P}^n$ converges to $\boldsymbol{P}$ under $d_{(\mathrm{G})}$ and continuity of the bijective mapping $\boldsymbol{\beta}$, we know that $\boldsymbol{\beta}(\boldsymbol{\alpha}^{\bar{\boldsymbol{P}}}) = \boldsymbol{\beta}(\boldsymbol{\alpha}^{\boldsymbol{P}})$. As long as the solution to (RI) is unique, this point can be written in a unique way as

a convex combination over $\boldsymbol{\beta}(\mathcal{A})$. This implies that the marginals $p^{n_k} = \sum_{i\in\mathcal{I}} \pi_i P_i^k$ converge to $p = \sum_{i\in\mathcal{I}} \pi_i P_i$.

As such, all convergent subsequences of the bounded sequence p^n converge to the same limit p^*. The Bolzano-Weierstrass theorem thus implies that p^n itself converges to p^*. By continuity of the first-order conditions (1), the convergence translates to the conditional choice defined in Equation (5). □

A.2 Algorithm description

A.2.1 Benchmark Routine

Our base routine for small to moderate menus works as follows: We make use of the scaling property (Lemma 1) to avoid floating point imprecision and store the normalized attention vectors in a I-by-$|\mathcal{A}|$ matrix with entries $B_{i\boldsymbol{a}} = \beta_i(\boldsymbol{a}) / \max_{\tilde{\boldsymbol{a}}\in\mathcal{A}} \beta_i(\tilde{\boldsymbol{a}})$. Starting with an initial guess for the marginals,[23] $\boldsymbol{p}^0$, we iteratively solve a second-order Taylor approximation to (G),[24] which after dropping constant terms yields

$$\boldsymbol{q}^k := \arg\max_{\boldsymbol{p}\in\Delta^{|\mathcal{A}|-1}} \frac{1}{2}\boldsymbol{p}^\intercal B^\intercal H B\boldsymbol{p} - 2\boldsymbol{\nabla} w(B\boldsymbol{p}^k)^\intercal B,$$

where H refers to the diagonal matrix with entries $H_{ii} = \pi_i/(B\boldsymbol{p}^k)_i^2$. When the objective function w is particularly flat, it can happen that this process 'overshoots' and results in attention vectors $\boldsymbol{b}^k = B\boldsymbol{p}^k$ and $\boldsymbol{b}' = B\boldsymbol{q}^k$ that are on opposite sides of the optimum, which can lead to long cycles. We can partially avoid this by making sure that $\boldsymbol{\nabla} w(\boldsymbol{b}') \cdot \boldsymbol{b}^k \leq 1$, which ensures that the bounding hyperplane imposed by the candidate $\boldsymbol{b}'$ points away from $\boldsymbol{b}^k$. If the inequality holds, we set $\boldsymbol{p}^{k+1} := \boldsymbol{q}^k$ and

[23] Practically, we use the full-information marginals by placing weight π_i on $\arg\max_{\boldsymbol{a}\in\mathcal{A}} a_i$.

[24] We implement this code using MATLAB's built-in quadprog solver (Version 2019b). Since the solver does not accept an initial guess, we use an equivalent centered problem by solving for $\boldsymbol{dp} = \boldsymbol{p} - \boldsymbol{p}^k$ instead.

move to the next iteration. Otherwise, we know that by strict convexity of w, there exists a point along the segment between $[\boldsymbol{b}^k, \boldsymbol{b}']$ that does better than both. In that case, we determine the candidate marginals $\boldsymbol{p}^{k+1} = t\boldsymbol{p}^k + (1-t)\boldsymbol{q}^k$ by identifying the root of the monotone function $\boldsymbol{\nabla} w(t\boldsymbol{p}^k + (1-t)\boldsymbol{q}^k) \cdot (\boldsymbol{q}^k - \boldsymbol{p}^k)$ where the indifference curve lies tangent to the segment.

We repeat this quadratic approximation until the implied IE converges, i.e. until $d_{(\mathrm{G})}(\boldsymbol{P}^k, \boldsymbol{P}^{k+1}) < \varepsilon$, where $\boldsymbol{P}^k$ is defined from $\boldsymbol{p}^k$ according to (1). As a default, and in all our applications, we use tolerance parameter $\varepsilon = 10^{-12}$. By construction, our approach ensures that the objective value $w(B\boldsymbol{p}^k)$ increases with each iteration.

When the action space is rich, the attention matrix B can require a lot of memory. To avoid this limitation, we first apply the base routine to a coarse subgrid of the menu, $\bar{A}^0 \subset \mathcal{A}$. Upon convergence, we denote the estimated marginals by $\boldsymbol{q}^0$, its associated attention vector as $\boldsymbol{b}^0 = B^0\boldsymbol{q}^0$, and the tentative consideration set as $A^0 = \mathsf{support}(\boldsymbol{q}^0)$. We then compute the $\boldsymbol{b}^0$-scores over a finer subgrid $\bar{A}^1 \supseteq \bar{A}^0$. We add the actions with the highest score to A^0 until the menu reaches some maximum cardinality K or contains all actions in some p-cover of grid $\bar{A}^1$. We repeatedly apply the base routine to obtain updated estimates $\boldsymbol{q}^{1,m}$, $\boldsymbol{b}^{1,m}$ and $\mathcal{A}^{1,m}$, and after each step we augment $\mathcal{A}^{1,m}$ with the actions in $\bar{A}^1$ that have the highest $\boldsymbol{b}^{1,m}$-scores. As long as K is large enough, the p-cover eventually stabilizes, and we move to the next finer subgrid $\bar{\mathcal{A}}^2$. We continue this process until the grid encompasses all of $\mathcal{A}$ and the p-cover stabilizes.

The provided code returns the estimated choice probabilities and computes partial covers at any desired probability level p, as described in Section 4.1. To identify dominated actions, we restrict the set of feasible optimal gradients Ψ as follows: First, we take the final numerical estimate $\boldsymbol{b}^0$, perturb it slightly along each dimension, and

consider the largest feasible attention vector along the perturbed ray.[25] Together, this yields a finite set of near-optimal solutions $\widehat{B} = \{\boldsymbol{b}^0, ..., \boldsymbol{b}^I\} \subset \mathcal{B}$. The optimality conditions in Theorem 1(b) imply that $\boldsymbol{\nabla} w(\boldsymbol{b}^k) \cdot \boldsymbol{b} \geq 1$ for all k, and thus restricts $\boldsymbol{b}^*$ to a small sub-region $\widehat{B} \subset \mathcal{B}$ that is obtained by imposing these additional inequality constraints. Since $\nabla_i w(\boldsymbol{b}) = \pi_i / b_i$ is strictly decreasing in b_i, we obtain the linear bounds

$$\nabla_i w(\boldsymbol{b}) \in \left[\frac{\pi_i}{\max_{\widehat{B}} b_i}, \frac{\pi_i}{\min_{\widehat{B}} b_i} \right]. \tag{8}$$

Moreover, the optimality conditions in Theorem 1(a) require that the gradient $\boldsymbol{\nabla} w(\boldsymbol{b}^*)$ satisfies the additional linear inequality constraints

$$\boldsymbol{v} \cdot \boldsymbol{\beta}(\boldsymbol{a}) \leq 1 \qquad \forall \boldsymbol{a} \in \mathcal{A}. \tag{9}$$

Together Equations (8) and (9) form a feasible polytope Ψ for the optimal gradient $\boldsymbol{\nabla} w(\boldsymbol{b}^*)$. Dominated actions can thus be identified as those with a negative maximal $\boldsymbol{b}^*$-score, i.e. those with $\max_{\boldsymbol{\psi} \in \Psi} \boldsymbol{\psi} \cdot \boldsymbol{\beta}(\boldsymbol{a}) - 1 < 0$.

A.2.2 Dynamic Variant

Miao and Xing [2022] tractably characterize the solution to their dynamic RI problem by constructing recursively defined value functions in two stages.[26] First, the state-dependent value of a particular action $\boldsymbol{a} \in \mathcal{A}$ is defined as the sum of the flow utility plus the discounted ignorance equivalent of the continuation problem

$$v_i^t(\boldsymbol{a}^t) = a_i^t + \beta \sum_{j \in \mathcal{I}} \Pi(j|i) \alpha_j^{t+1}(\boldsymbol{a}^t), \tag{10}$$

[25] Formally, we solve $\max_{k \in \mathbb{R}, \boldsymbol{b} \in \mathcal{B}} k$ subject to $\boldsymbol{b} \geq k(\boldsymbol{b}^0 + \varepsilon \boldsymbol{e}^i)$, where $\varepsilon > 0$ is a small perturbation scalar and $\boldsymbol{e}^i$ denotes the unit vector in dimension i.

[26] Steiner et al. [2017] take a similar approach.

where $\Pi(j|i)$ denotes the exogenously given probability that the state transitions from i to j, β is the discount factor, and $\boldsymbol{\alpha}_j^{t+1}(\boldsymbol{a}^t)$ denotes the ignorance equivalent of the continuation problem that ensues under the posteriors associated with action $\boldsymbol{a}^t$. The ignorance equivalent in turn is determined from the choice probabilities in the subsequent periods, dating back to Caplin et al. [2018] and generalized in Müller-Itten et al. [2023],

$$\alpha_i^t(\boldsymbol{a}^{t-1}) = \lambda \ln \left(\sum_{\boldsymbol{a}^t \in \mathcal{A}} p^t(\boldsymbol{a}^t|\boldsymbol{a}^{t-1}) \exp\left(v_i^t(\boldsymbol{a}^t)/\lambda\right) \right), \tag{11}$$

where $p^t(\boldsymbol{a}^t|\boldsymbol{a}^{t-1})$ denotes the agent's marginal likelihood of selecting action $\boldsymbol{a}^t$ conditional on the belief induced by $\boldsymbol{a}^{t-1}$ in the previous period.[27] It can also be obtained from the optimal attention vector as $\alpha_i^t(\boldsymbol{a}^{t-1}) = \lambda \ln\left(b_i^t(\boldsymbol{a}^{t-1})\right)$,

Miao and Xing [2022] propose a clever 'forward-backward' algorithm that works as follows. Starting from an initial (sub-optimal) guess regarding optimal information acquisition behavior, $P_i^t(\boldsymbol{a}^t)$, one can iterate *forward* to determine the resulting probability distributions and beliefs for any history. In each period, this associates to each action an endogenous posterior belief that is used as the prior in the subsequent period. With these beliefs in hand, one can then iterate *backwards* to determine the optimal behavior after each history, and compute the continuation values using Equations (10) and (11). With new guesses for the optimal behavior in hand, one can again iterate forward to determine beliefs and backwards to infer behavior, until convergence.

During the backwards iteration, Miao and Xing [2022] employ the Blahut-Arimoto conditions and argue that this is guaranteed to converge to the optimum because of

[27] We here focus on Markov strategies, but the expression could be generalized to allow for arbitrary dependence of of p (and Π) on the past history, as outlined in Miao and Xing [2022].

the convexity of the underlying problem. Since the GAP-SQP algorithm converges more quickly than BA in static settings, it is thus tempting to replace this BA step with a single iteration of the quadratic approximation.

Algorithm Specification. At each iteration k, the algorithm computes a guess for the optimal choice, described by the conditionals $P_i^{k,t}(\boldsymbol{a}^t|\boldsymbol{a}^{t-1})$ and the marginals $p^{k,t}(\boldsymbol{a}^t|\boldsymbol{a}^{t-1})$. In terms of outcome distributions, the algorithm also maintains a guess for the joint distribution $\mu_i^{k,t}(\boldsymbol{a}^{t-1})$ of the period-t state i and the previous action $\boldsymbol{a}^{t-1}$ and the prior beliefs associated with each history, $\boldsymbol{\pi}^{k,t}(\boldsymbol{a}^{t-1}) \in \Delta\mathcal{I}$. Finally, the algorithm keeps track of a guess for the continuation values $v_i^{k,t}(\boldsymbol{a}^t)$ and the optimal attention vectors $b_i^{k,t}(\boldsymbol{a}^{t-1})$.

We initialize the algorithm with the full-information guess for the state-contingent choice rule, $P_i^{0,t}(\boldsymbol{a}^t|\boldsymbol{a}^{t-1}) = 1$ for the first action that maximizes $\max_{\boldsymbol{a}\in\mathcal{A}} a_i$, and $P_i^{0,t}(\boldsymbol{a}^t|\boldsymbol{a}^{t-1}) = 0$ otherwise. We also initialize all beliefs to the initial time-zero beliefs of the agent, $\boldsymbol{\pi}^{0,t}(\boldsymbol{a}^{t-1}) \equiv \boldsymbol{\pi}^0$. We then proceed starting with iteration $k = 1$ as follows.

Forward Step. Starting with period $t = 1$, we update our guesses for joint distributions and beliefs in each subsequent period:

(a) For period $t = 1$, the joint distribution is obtained simply by assuming that all conceivable (and counterfactual) time-zero histories are equally likely, $\mu_i^{k,1}(\boldsymbol{a}^0) \equiv \frac{1}{|\mathcal{A}|}\pi_i$ for all $\boldsymbol{a}^0$, where $\boldsymbol{\pi}$ denotes the agent's initial prior. This distribution remains unchanged across all iterations k of the algorithm.

(b) For each subsequent period $t + 1$, the joint distribution can be inferred from the law of total probabilities across all combinations of the period-t

state i and the preceding action $\boldsymbol{a}^{t-1}$,

$$\mu_j^{k,t+1}(\boldsymbol{a}^t) = \sum_{i\in\mathcal{I}} \sum_{\boldsymbol{a}^{t-1}\in\mathcal{A}} \Pi(j|i) P_i^{k,t}(\boldsymbol{a}^t|\boldsymbol{a}^{t-1}) \mu_i^{k,t}(\boldsymbol{a}_{t-1}). \tag{12}$$

(c) From these joint distributions, one can back out the prior beliefs at each period by the law of conditional probabilities,

$$\pi_i^{k,t}(\boldsymbol{a}^{t-1}) = \frac{\mu_i^{k,t}(\boldsymbol{a}^{t-1})}{\sum_{j\in\mathcal{I}} \mu_j^{k,t}(\boldsymbol{a}^{t-1})} \tag{13}$$

provided that the denominator is nonzero. If the denominator is zero, we simply maintain the beliefs from the previous iteration, $\pi_i^{k,t}(\boldsymbol{a}^{t-1}) = \pi_i^{k-1,t}(\boldsymbol{a}^{t-1})$.

Backward Step. Starting with period T, we update our guesses for continuation values and determine optimal choices in each previous period:

(d) We initialize the period $T+1$ attention vectors to $b_i^{k,T+1}(\boldsymbol{a}^T) = 0$, corresponding to an ignorance equivalent of $\lambda \ln(b_i^{k,T+1}) \equiv \mathbf{0}$.

(e) Beginning with period $t = T$, we determine the continuation value according to Equation (10),

$$v_i^{k,t}(\boldsymbol{a}^t) = a_i^t + \beta \sum_{j\in\mathcal{I}} \Pi(j|i) \lambda \ln(b_j^{k,t+1}(\boldsymbol{a}^t)). \tag{14}$$

(f) Using the payoffs $\left\{v_i^{k,t}(\boldsymbol{a})\right\}_{\boldsymbol{a}\in\mathcal{A}}$ and the belief $\pi_i^{k,t}(\boldsymbol{a}^{t-1})$, we determine the optimal marginals, attention vector and conditional choice probabilities.

BA. In the BA variant, we perform a single iteration of the Blahut-

Arimoto algorithm,

$$p^{k,t}(\boldsymbol{a}^t|\boldsymbol{a}^{t-1}) = \sum_{i\in\mathcal{I}} \pi_i^{k,t}(\boldsymbol{a}^{t-1}) P_i^{k,t}(\boldsymbol{a}^t|\boldsymbol{a}^{t-1}) \tag{15}$$

$$b_i^{k,t}(\boldsymbol{a}^{t-1}) = \sum_{\boldsymbol{a}\in\mathcal{A}} p^{k,t}(\boldsymbol{a}^t|\boldsymbol{a}^{t-1}) \exp(v_i^{k,t}(\boldsymbol{a}^t)/\lambda) \tag{16}$$

$$P_i^{k,t}(\boldsymbol{a}^t|\boldsymbol{a}^{t-1}) = p^{k,t}(\boldsymbol{a}^t|\boldsymbol{a}^{t-1}) \frac{\exp(v_i^{k,t}(\boldsymbol{a}^t)/\lambda)}{b_i^{k,t}(\boldsymbol{a}^{t-1})}. \tag{17}$$

GAP-SQP. In the GAP-SQP variant, we instead obtain $p^{k,t}(\boldsymbol{a}^t|\boldsymbol{a}^{t-1})$ by calling GAP-SQP for a single iteration, using $p^{k-1,t}(\boldsymbol{a}^t|\boldsymbol{a}^{t-1})$ as the initial guess.[28] We then infer the optimal attention vector and conditional choice probabilities using the formulas described in Section 3, slightly perturbing the conditionals with a small $\varepsilon > 0$ to ensure that beliefs are updated everywhere,

$$b_i^{k,t}(\boldsymbol{a}^{t-1}) = \sum_{\boldsymbol{a}\in\mathcal{A}} p^{k,t}(\boldsymbol{a}^t|\boldsymbol{a}^{t-1}) \exp(v_i^{k,t}(\boldsymbol{a}^t)/\lambda) \tag{18}$$

$$P_i^{k,t}(\boldsymbol{a}^t|\boldsymbol{a}^{t-1}) = \frac{\left((1-\varepsilon)p^{k,t}(\boldsymbol{a}^t|\boldsymbol{a}^{t-1}) + \frac{\varepsilon}{|\mathcal{A}|}\right) \exp(v_i^{k,t}(\boldsymbol{a}^t)/\lambda)}{\sum_{\boldsymbol{a}'\in\mathcal{A}} \left((1-\varepsilon)p^{k,t}(\boldsymbol{a}'|\boldsymbol{a}^{t-1}) + \frac{\varepsilon}{|\mathcal{A}|}\right) \exp(v_i^{k,t}(\boldsymbol{a}')/\lambda)}. \tag{19}$$

Repeat. We increase the iteration to $k+1$ and repeat until convergence.

Since our current goal is to compare the performance of the two subroutines, we terminate the both approaches after a set amount of time. In applications where the primary goal is to estimate the behavior in a dynamic RI problem, we suggest a stopping criteria based on the following factors:

- Attention-vector distance, d_β, across iterations for all histories. This is akin

[28] In iteration 1, we obtain the initial guess for $p^{1,t}(\boldsymbol{a}^t|\boldsymbol{a}^{t-1})$.

to value-vector convergence proposed by Miao and Xing [2022], but has the added benefit that it guarantees convergence to the optimal conditional choice probabilities (see Lemma 2).

- Distance in implied beliefs at each history across iterations. This is the implicit condition on which the forward-backward approach of both algorithms rely.

- The maximal sufficiency score $\max_{t,\boldsymbol{a}^t,\boldsymbol{a}^{t-1}} s^{k,t}(\boldsymbol{a}^t|\boldsymbol{a}^{t-1})$ across all histories, where

$$s^{k,t}(\boldsymbol{a}^t|\boldsymbol{a}^{t-1}) = \sum_{i\in\mathcal{I}} \pi_i^{k,t}(\boldsymbol{a}^{t-1}) \frac{\exp(v_i^{k,t}(\boldsymbol{a}^t)/\lambda)}{b_i^{k,t}(\boldsymbol{a}^{t-1})}$$

  in line with Section 4.1.

When all three of these measures are close to zero, the researcher can be confident that the guess not only achieves near-optimal welfare overall, it also approximates the optimal behavior at all Markov histories.

References

Dirk Bergemann and Stephen Morris. Bayes correlated equilibrium and the comparison of information structures in games. *Theoretical Economics*, 11(2):487–522, 2016. doi: https://doi.org/10.3982/TE1808. URL https://onlinelibrary.wiley.com/doi/abs/10.3982/TE1808.

Simone Bertoli, Jesús Fernández-Huertas Moraga, and Lucas Guichard. Rational inattention and migration decisions. *Journal of International Economics*, 126:103364, 2020. ISSN 0022-1996. doi: https://doi.org/10.1016/j.jinteco.2020.103364. URL https://www.sciencedirect.com/science/article/pii/S0022199620300805.

Zach Y. Brown and Jihye Jeon. Endogenous information and simplifying insurance choice. *Unpublished working paper*, 2023.

Andrew Caplin, Mark Dean, and John Leahy. Rational inattention, optimal consideration sets, and stochastic choice. *Review of Economic Studies*, 86(3):1061–1094, 07 2018. ISSN 0034-6527. doi: 10.1093/restud/rdy037. URL https://doi.org/10.1093/restud/rdy037.

Thomas M Cover and Joy A Thomas. *Elements of information theory*. John Wiley & Sons, 2012.

Kunal Dasgupta and Jordi Mondria. Inattentive importers. *Journal of International Economics*, 112(C):150–165, 2018. doi: 10.1016/j.jinteco.2018.03. URL https://ideas.repec.org/a/eee/inecon/v112y2018icp150-165.html.

Harold Gordon Eggleston. *Convexity*. Cambridge Tracts in Mathematics. Cambridge University Press, 1958. doi: 10.1017/CBO9780511566172.

Xavier Gabaix. A sparsity-based model of bounded rationality. *Quarterly Journal of Economics*, 129(4):1661–1710, 2014.

Wagner Piazza Gaglianone, Raffaella Giacomini, João Victor Issler, and Vasiliki Skreta. Incentive-driven inattention. *Journal of Econometrics*, 2020.

Lixin Huang and Hong Liu. Rational inattention and portfolio selection. *Journal of Finance*, 62(4):1999–2040, 2007. ISSN 00221082, 15406261. URL http://www.jstor.org/stable/4622323.

Kenneth Judd. *Numerical Methods in Economics*, volume 1. The MIT Press, 1 edition, 1998. URL https://EconPapers.repec.org/RePEc:mtp:titles:0262100711.

Junehyuk Jung, Jeong Ho (John) Kim, Filip Matějka, and Christopher A. Sims. Discrete actions in information-constrained decision problems. *Review of Economic Studies*, 03 2019. ISSN 0034-6527. doi: 10.1093/restud/rdz011. URL https://doi.org/10.1093/restud/rdz011. rdz011.

Marcin Kacperczyk, Stijn Van Nieuwerburgh, and Laura Veldkamp. A rational theory of mutual funds' attention allocation. *Econometrica*, 84(2):571–626, 2016.

Yulei Luo, Jun Nie, Gaowang Wang, and Eric R. Young. Rational inattention and the dynamics of consumption and wealth in general equilibrium. *Journal of Economic Theory*, 172:55 – 87, 2017. ISSN 0022-0531. doi: https://doi.org/10.1016/j.jet.2017.08.005. URL http://www.sciencedirect.com/science/article/pii/S0022053117300832.

Bartosz Maćkowiak and Mirko Wiederholt. Optimal sticky prices under rational inattention. *American Economic Review*, 99(3):769–803, 2009. ISSN 00028282, 19447981. URL http://www.jstor.org/stable/25592482.

Bartosz Maćkowiak and Mirko Wiederholt. Information processing and limited liability. *American Economic Review*, 102(3):30–34, May 2012. doi: 10.1257/aer.102.3.30. URL http://www.aeaweb.org/articles?id=10.1257/aer.102.3.30.

Bartosz Maćkowiak, Filip Matějka, and Mirko Wiederholt. Rational inattention: A review. *Journal of Economic Literature*, 61(1):226–273, 2023.

Filip Matějka. Rationally inattentive seller: Sales and discrete pricing. *Review of Economic Studies*, 83(3):1125–1155, 2016.

Filip Matějka and Alisdair McKay. Rational inattention to discrete choices: A new foundation for the multinomial logit model. *American Economic Review*, 105(1):

272–98, January 2015. doi: 10.1257/aer.20130047. URL http://www.aeaweb.org/articles?id=10.1257/aer.20130047.

Jianjun Miao and Hao Xing. Dynamic disrete choice under rational inattention. Working paper, Boston University, May 2022.

Jianjun Miao, Jieran Wu, and Eric Young. Multivariate rational inattention. *Econometrica*, 90(2):907–945, March 2022.

Jordi Mondria. Portfolio choice, attention allocation, and price comovement. *Journal of Economic Theory*, 145(5):1837–1864, 2010.

Michèle Müller-Itten, Roc Armenter, and Zachary Stangebye. Rational inattention via ignorance equivalence. Working paper, Philadelphia Fed WP 21-29, 2023.

Lin Peng. Learning with information capacity constraints. *Journal of Financial and Quantitative Analysis*, 40(2):307–329, 2005. ISSN 00221090, 17566916. URL http://www.jstor.org/stable/27647199.

Lin Peng and Wei Xiong. Investor attention, overconfidence and category learning. *Journal of Financial Economics*, 80(3):563 – 602, 2006. ISSN 0304-405X. doi: https://doi.org/10.1016/j.jfineco.2005.05.003. URL http://www.sciencedirect.com/science/article/pii/S0304405X05002138.

Christopher A. Sims. Implications of rational inattention. *Journal of Monetary Economics*, 50(3):665–690, 2003.

Christopher A. Sims. Rational inattention: Beyond the linear-quadratic case. *American Economic Review*, 96(2):158–163, 2006.

Jakub Steiner, Colin Stewart, and Filip Matějka. Rational inattention dynamics: Inertia and delay in decision-making. *Econometrica*, 85(2):521–553, 2017.

George Tauchen. Finite-state markov chain approximations to univariate and vector autoregressions. *Economics Letters*, 20:177–181, 1986.

Stijn Van Nieuwerburgh and Laura Veldkamp. Information immobility and the home bias puzzle. *Journal of Finance*, 64(3):1187–1215, 2009. doi: 10.1111/j.1540-6261.2009.01462.x. URL https://onlinelibrary.wiley.com/doi/abs/10.1111/j.1540-6261.2009.01462.x.

Stijn Van Nieuwerburgh and Laura Veldkamp. Information acquisition and under-diversification. *Review of Economic Studies*, 77(2):779–805, 2010.